SOUTHERN BOUNDARY RESTORATION AND ENHANCEMENT FUND PROJECT FINAL REPORT

A study to determine the feasibility of hydroacoustic monitoring of migrating sockeye and pink salmon in the marine area

Svein Vagle[1], Li Ding[2], Mari Boesen[3], George Cronkite[4] and Yunbo Xie[5]

[1]Fisheries and Oceans Canada, Institute of Ocean Sciences
[2]Vitech. Vitech Innovative Research & Consulting, Richmond, BC, Canada
[3]University of Victoria, Victoria, BC
[4]Fisheries and Oceans Canada, Pacific Biological Station
[5]Pacific Salmon Commission, Vancouver, BC

April 2008

ABSTRACT

With a decreasing availability of the important catch per unit effort data from purse seine test fisheries in both Juan de Fuca and Johnstone Straits there is an urgent need to develop alternative ways to obtain accurate and timely information on migration abundance and behaviour of salmon returning to the Fraser River from marine waters; information that the management of the sockeye salmon fisheries relies on. To assess the possibility of using fixed cabled to shore hydro-acoustic systems, a tripod with two backscatter sonars (12 and 100 kHz) was deployed at Chatham Pt. lighthouse station in southern Johnstone Strait for four months between July and October 2007. The medium range 12 kHz sonar was used to cover the main part of the 1.6 km wide channel from between 50 and about 800 m and the 100 kHz system covered the 6 to 200 m range. The tendency for pink salmon to travel closer to shore than the sockeye salmon might give us an opportunity to separate targets based on range. A sound propagation model for the area plus target tracking algorithms were developed for the processing and interpretation of the acoustical backscatter data. The results show that there is agreement between these acoustical abundance estimates and fish count estimates from the Fraser River at Mission. However, careful system calibrations are required to assess the absolute ability of the Chatham Pt. system for abundance estimates. A DIDSON imaging sonar was also used at the site in an attempt at detecting and counting fish in the marine environment. The DIDSON system did provide some useful information, but that in an ongoing enumeration facility the time required to gain useful data may not be well spent. The system may be of most use during the peaks of migration and as a tool to investigate targets detected by the 12 and 100 kHz systems, and perhaps to identify species composition. The overall conclusion of the study is that the use of fixed location, cabled to shore, sidescan sonar systems represent a novel approach to obtain the critical information on migration abundance of salmon returning to the Fraser River.

TABLE OF CONTENTS

INTRODUCTION

The management of Fraser River sockeye salmon fisheries relies on accurate and timely information on migration abundance and behavior of salmon returning to the river from marine waters. The presence of Vancouver Island at the entrance to the Fraser River limits the river entrances of all returning salmon to two marine approaches: a narrow 2km wide by 300m deep channel (southern Johnstone Strait) in the north (Fig. 1) and a somewhat wider (approximately 20km) but shallower (~200m) channel to the south (Strait of Juan de Fuca). The required information is primarily estimated from catch per unit effort (CPUE) data from purse seine test fisheries in both Juan de Fuca and Johnstone Straits. As a sampling method, test fishing is time and space limited, resulting in patchy information on migration and behavior of returning stocks. For example, on Aug. 23, 2006, the catch estimate in the purse seine test fishery in upper Johnstone Strait (Area 12) was 110,800 by **2** boats for a total of **12** sets. This was a "guesstimate" based on the experience of the fishing crews. Expansion of these CPUE data depends on the key assumption that catch ability (q) is well understood, i.e. uncertainty is modest and captured in the historical data. This assumption was likely severely violated in 2006. However, these observations have considerable weight on the in-season estimates of abundance of sockeye and pink salmon before they enter the river and pass the sonar counting station at Mission, B.C. Therefore, the in-season run-size estimates based on the marine areas CPUE data has a profound influence on subsequent fishery management actions.

Hydroacoustic technology provides an alternative approach that can sample a large volume of the water column on a continuous basis. The Pacific Salmon Commission (PSC) has successfully applied this technology to in-river estimation of daily salmon passage in the lower Fraser River near Mission, B.C. since 1977 (Banneheka et al. 1995, Xie et al. 2005) and the use of rotating sidescan sonar to detect near-surface fish has already been shown to be a viable approach for continuous fish monitoring (e.g., Trevorrow, 2001). If we were able to detect and count the returning salmon in southern Johnstone Strait and in the Strait of Juan de Fuca, this information would aid fisheries managers to make timely in-season decisions in meeting multiple objectives with regard to management and conservation issues to fulfill the obligations laid out in the Pacific Salmon Treaty.

During the summer and fall of 2007 we conducted a field study using state-of-the-art sonar systems deployed at Chatham Point lighthouse station in southern Johnstone Strait, combined with the development of novel data processing algorithms to determine whether acoustical monitoring of migrating salmon in the marine environment was feasible.

The overreaching goal of this work is to eventually provide reliable monitoring and estimates of arrival timing and abundance of Fraser River sockeye and pink salmon as they migrate through marine areas. This information will aid fisheries managers to make timely in-season decisions in meeting multiple objectives with regard to management and achievement of escapement or harvest rate targets.

This study focussed on seven objectives:

1. Locate a suitable site for deploying a cabled sonar system in Johnstone Strait during the sockeye and pink migration season;
2. Develop a propagation model for the proposed hydroacoustic system configuration based on local oceanographic data. This model will aid interpretation and analyses of acquired salmon flux data;
3. Compare 12 kHz and 100 kHz backscatter measurements with simultaneous DIDSON observations to establish whether these backscatter sonars are viable tools for monitoring of returning sockeye and pink salmon;
4. Develop a signal processing software package to allow automatic identification of fish targets from acquired echo data from both 12 and 100 kHz sonar systems;
5. Develop a fish-flux model to derive hourly and daily flux estimates of fish abundance migrating through the monitoring area from acoustically sampled fish targets;
6. Develop a methodology that combines the test-fishing based species composition data with the acoustically estimated total daily fish flux to derive daily sockeye and pink salmon abundance;
7. Compare the results with other sources of information, especially daily estimates of in-river salmon passages from the PSC Mission hydroacoustic station, to evaluate the performance of the proposed system and identify potential sources of bias.

This final report describes the study, the data, and analyses and findings pertaining to these objectives.

CHATHAM POINT LIGHTHOUSE STATION: THE STUDY SITE

We had four main requirements when deciding where to deploy a cabled sonar system for salmon migration tracking: 1) The location had to be where a majority, or preferably all, salmon of interest could be detected; 2) The site had to be accessible by road, for logistical and cost reasons; 3) There had to be access to electrical power for running sonar systems and associated computers and electronics; and 4) the geography and near shore bathymetry had to be suitable for deployment of a sonar tripod within reasonable distance to power and a shelter for the computer control and sonar electronics. In addition to these requirements we hoped to establish internet access at the site for remote control of the instrumentation and to simplify the transfer of data in a timely fashion.

After research which included discussions with local experts and colleagues that had worked in this area, we found the ideal location for this study at the Canadian Coast Guard lighthouse station at Chatham Point (50^{o} 19.842N 125^{o} 26.324W) in southern Johnstone Strait (Fig. 1). According to local fishermen, the returning salmon swim along the west side of the strait (along Vancouver Island) until they reach Chatham Pt. where the width of Johnstone Strait between the Point and East Thurlow Island is approximately 1.6 km. Here they cross over to the eastern side of the channel (mainland side, width 2.2 km) and then follow this side southwards (Fig. 1(b)). Most of the migration past Chatham Pt. takes place during the flood tides, at which time the current flows southwards.

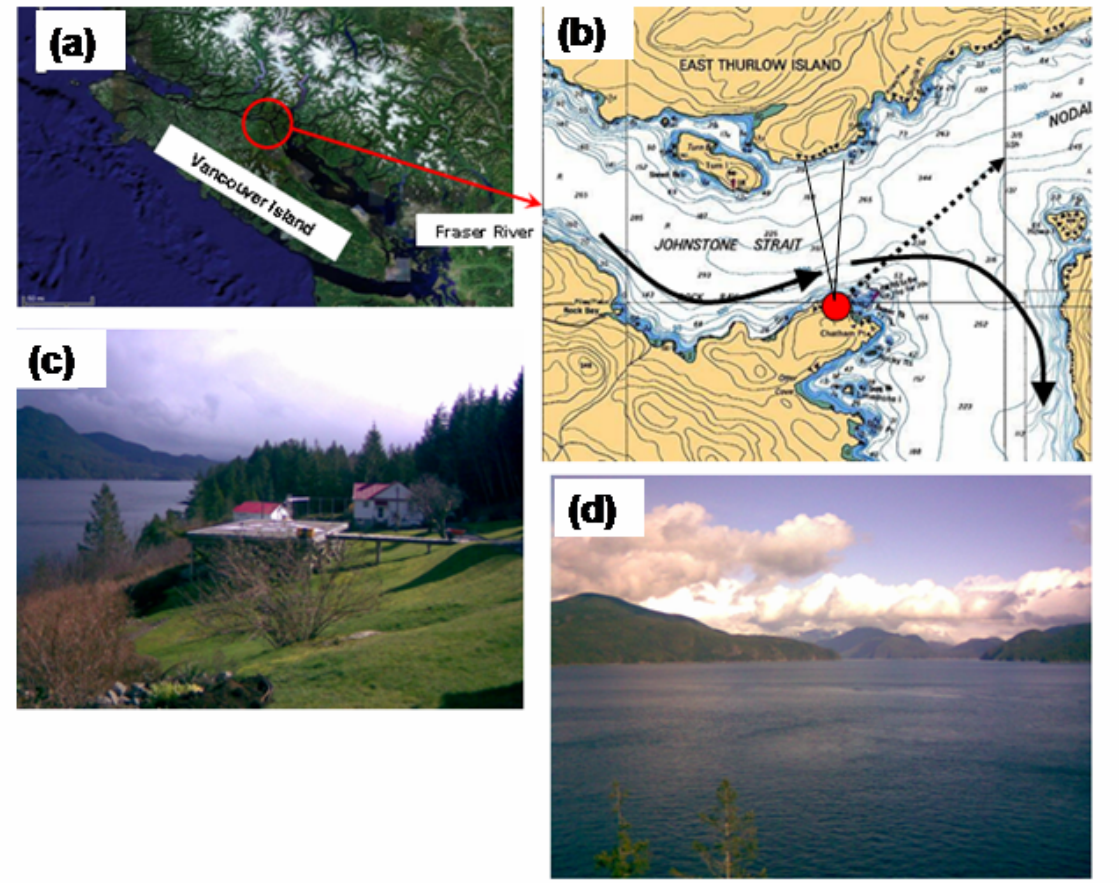

Fig. 1. Panels (a) & (b) show location of Chatham Point lighthouse station in Southern Johnstone Strait, Vancouver Island. The black arrows indicate the suspected main salmon migration route. (c) Shows the lighthouse station from the small building used to house the sonar electronics and data logging computer. The black dotted arrow in (b) shows the direction of the photograph in (d) and the solid thin lined wedge indicate the direction of the 12 kHz sonar beam.

The site is accessible by car via approximately 50 km of logging roads of variable condition. During our study, the area around the lighthouse station was actively logged, causing delays and resulting in periods when the access road was in very poor condition, requiring the use of 4-wheel drive vehicles.

Chatham Pt. lighthouse station has a generator running 24h per day to operate the lighthouse and the residences on the property and the Coast Guard allowed us access to this power to run our system for the duration of the study. There were voltage variations in the power supply that caused problems by rebooting our computer, but this problem was solved by installing an uninterrupted power supply (UPS).

We were concerned that there might not be suitable locations near the shoreline to deploy the instrumentation because of the steep rocky coastline at Chatham Point. However, the lighthouse keeper and local fishermen informed us that there was a shelf at approximately 15 m depth at the north end of the Pt. which would be suitable for our tripod. From this site cables were routed up the steep bank, approximately 100 m, to the small building, containing the lighthouse station fog horn and other assorted equipment (Fig. 2).

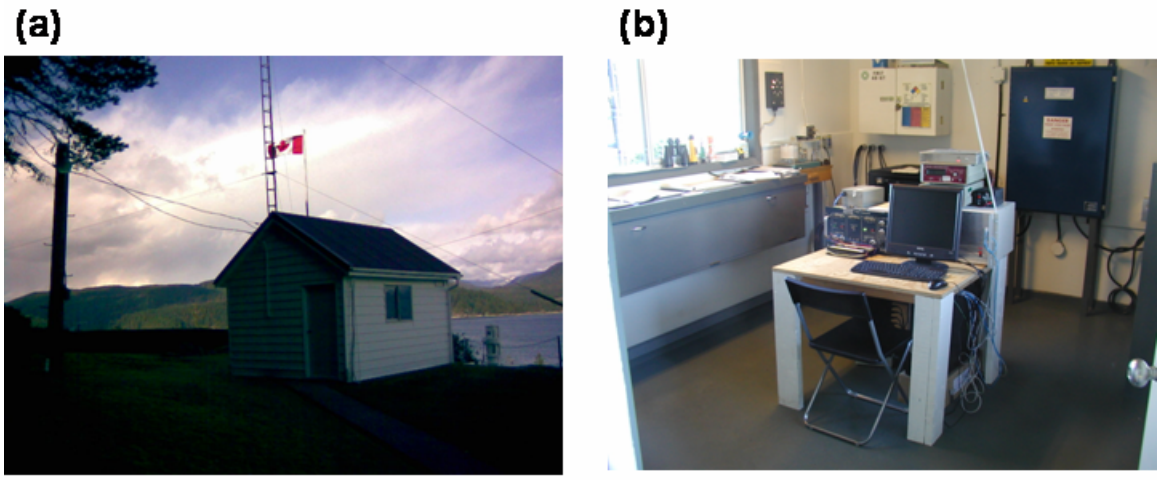

Fig. 2. (a) Chatham Pt. lighthouse station building used to store sonar electronics, logging and control computer and internet connection (b). Cables from the underwater sonar system were routed up the steep hill at the back of the building and through an existing conduit.

Initially we had planned to have personnel stationed near the site during the summer to operate the instrumentation and download data. However, site access was difficult and because it turned out that the lighthouse keeper had satellite internet access, we decided to connect the sonar system directly to the internet. We upgraded the internet link to the highest speed possible for the duration of the study. This allowed us to have real-time access to the sonar systems. However, it turned out that the link was neither reliable nor fast enough to transfer significant amounts of data. We therefore made four site visits over the season to retrieve the data. Nevertheless, the internet access was an advantage because it allowed us to verify that the system was working and sonar parameters could be changed when required.

THE CHATHAM POINT TRIPOD

The Tripod

The underwater part of the Chatham Pt. system consisted of a 1.5 m tall tripod on which we mounted a 40-element, 2.5 m long 12 kHz sonar array and a smaller array of 4 near orthogonal 100 kHz sidescan sonars (Fig. 3). The 12 kHz sonar array and the 100 kHz sidescan sonar transducers were mounted on two separate rotators so that they could be rotated independently in 104 and 304 degree sectors, respectively. The reason for this was to allow for steering following deployment so as to get the sonars to point in the desired direction. We also had plans to run the system in different configurations where the sonars would be pointing in different directions at different preset times. Both these rotators failed shortly after deployment due to severe corrosion. However, they lasted long enough to allow us to point the sonars in near optimum directions (Fig. 8).

The compasses on the two rotators were intended to give the direction of each sonar beam while rotating. These compasses and the associated tilt sensors also failed shortly after deployment. However, the tilt sensors were crucial during deployment to make sure that we had managed to deploy the tripod on a flat spot on the bottom. During deployment it quickly became apparent that the underwater shelf where we

intended to deploy the tripod was not as level as first anticipated. It took up to 4 tries plus extension of the adjustable leg before the tripod was deployed within an acceptable 3^{o} of horizontal. The tripod ended up in a location approximately 30 m from shore with a nominal water depth of 18 m.

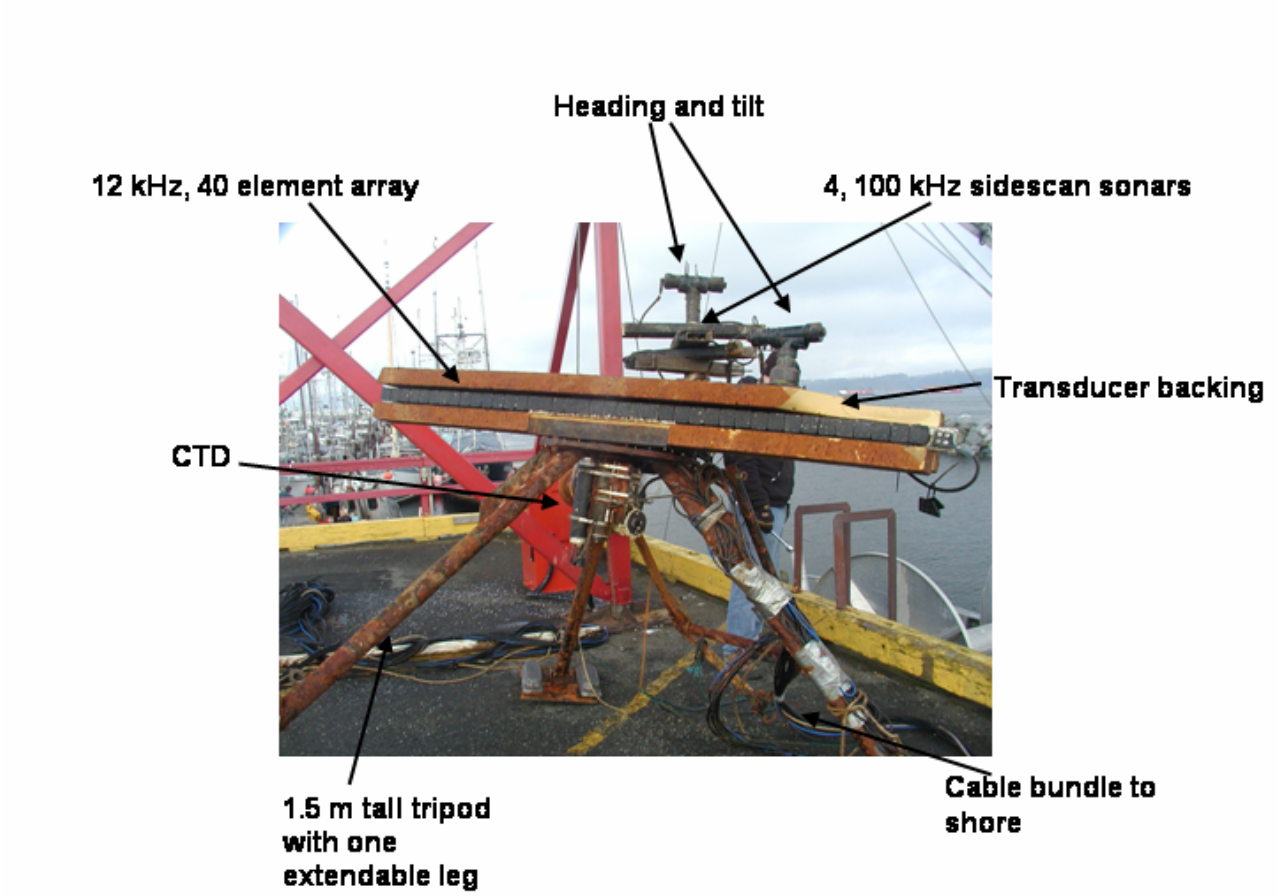

Fig. 3. Chatham Pt. tripod with sensors on government dock in Campbell River.

The tripod with all its sensors was assembled on the government wharf in Campbell River June 20-21 and deployed by Ken and Elvis Chickite on June 21 from the seine boat Marinet who were chartered for the task (Fig. 4). Ken and Elvis did an excellent job during both deployment and recovery of the tripod. Their boating skills under less than ideal conditions right next to the rocks at Chatham Pt. were amazing.

The cable bundle consisting of 10 individual cables was pulled up the steep bank from the beach and connected to the electronics and computer inside the small lighthouse station building approximately 100 m away. Following approximately 4 months in the water the tripod was recovered by the crew on the Marinet on November 23rd, 2007.

Fig. 4. The seine boat Marinet departing Campbell River for Chatham Pt. June 21, 2007 with the tripod onboard.

12 kHz intermediate-range sonar

Side looking sonars have the potential for fish detection within horizontal ranges of several kilometres, providing spatial coverage several orders of magnitude greater than conventional vertical ship-based echo-sounders or conventional test fishery net trawls. In this work we explored the feasibility of using a 12 kHz sidescan sonar for fish detection across Johnstone Strait. The range of approximately 1.6 km across the strait is considered as an intermediate range, lying between ranges accessible to more commonly used high (~100 kHz) and low (~1 kHz) sonar systems (Farmer et al., 1999).

The sonar system used here consisted of a 40-element (20λ) 12 kHz sidescan array connected to an EDO/Western model 248 Sonar Transceiver. The 12 kHz operating frequency is a good compromise between low acoustic absorption while maintaining transducer directivity at manageable physical size. It also turns out that 12 kHz is a frequency less sensitive to bubbles injected by breaking waves during windy conditions, turbulence during strong tidal currents, and ship wakes. The array length is 2.49 m giving a one-way horizontal beam width of 2.8° (to -3 dB), with a vertical beam-width of 122° and front to back ratio of approximately -20 dB (one way) with an installed 75 mm thick epoxy foam material behind the transducer (Fig. 3). The far-field on-axis output power source level of the system was approximately 210 dB re 1 μPa. The transceiver was modified to accept externally generated pulses (software generated). The system was also capable of transmitting linear frequency modulated sweeps of duration up to 200 ms, but due to concerns with regards to noise impact on marine mammals we only transmitted simple 12 kHz pulses of up to 10 ms in length. Following a time-varied gain (TVG) amplifier, the received signals were digitized at 48 kHz and processed in a digital signal processing (DSP) chip before being sent to a PC for storage and real-time display. The range resolution was approximately 2 m for a transmitted pulse-width of 3 ms, which was used for most of the data acquisition with this sonar system. For most of the experiment we transmitted once every 2 seconds resulting in a maximum sounding range of approximately 1500 m. The shortest range at which this system can be used is defined by the transition from near-field to far-field of the array. From the commonly used definition of the start of the far-field, $r_f=R^2/\lambda$, where R is the largest dimension of the array and λ is the acoustic wavelength, we get approximately 50 m for the 12 kHz system.

(For comparison, the corresponding range for the 100 kHz system, described in the next section, is approximately 6 m.) The system was intended for 24 h/day operation.

4-channel 100 kHz sidescan sonar system

For near shore (<~200 m) measurements we deployed a system consisting of 4, 100 kHz sidescan transducers mounted so that each of them was pointing 45^o apart, covering 180^o (Fig. 8). These sidescan transducers have fan shaped beams 3^o by 60^o (to -3dB), with maximum sidelobes at -24 dB. The transducers were connected to transceiver capable of providing approximately 500 W (electrical) to each transducer which were synchronized to transmit together. This output power corresponds to on-axis source level of roughly 215 dB re 1 μPa. A pulse length of 0.5 ms was used, yielding range resolution of 37 cm at a pulse to pulse transmission rate of 2Hz.

The system was controlled by a PC which digitized the received signal following a time-varied gain (TVG), displayed the data in real time and stored the data to disk. This system operated for nearly 4 months and generated more than 500 Gbytes of data.

Real-time internet system control

Both the 12 kHz intermediate range sonar system and the 4-channel 100 kHz system were controlled in real-time using internet controls. The building housing the sonar electronics was connected to the main lighthouse station house via a directional wireless network and connected to the satellite internet connection in the house. Real time displays from both systems were available at the Institute of Ocean Sciences 24 h/day. Software on the systems could be updated and modified without having to make the 6h drive to the lighthouse station. Some data could be downloaded but the bandwidth of the system was not suitable for transfer of the large acoustical data sets on a routine basis, even though the internet provider claimed their system was capable.

For any future long-term operation it will probably not be required to store all the raw data, so this limitation should not be an issue.

THE DIDSON SYSTEM

The DIDSON sonar operates in a mega-hertz frequency range of 1.1 and 1.8 MHz in detection and identification modes, respectively. The sonar insonifies fish with a large azimuthal composite beam of 29^o as shown in Fig. 5. When operating in 1.8-MHz detection mode, this composite beam is formed by 96 fan-shaped narrow beams. Each of the 96 individual beams has dimensions of 0.3^o by 14^o. The system utilises multiple sound beams focused through a moveable lens to produce near video quality images comprised of frames produced by the 96 beams. A frame (image) is constructed in sequence and consists of 8 sets of 12 beams fired simultaneously. The composite beam with an angular field of view of 29^o × 14^o, provides not only a complete coverage of the entire body of a typical salmon target but also a range-dependent azimuthal resolution for the body shape of imaged fish. For example, at a 10-m range, the composite beam provides approximately 5m × 2m rectangular imaging area, which is more than adequate for insonifying the entire body length of a typical adult sockeye. The resulting image of the fish has a 2-cm resolution along the

azimuthal direction of the composite beam. In comparison, a 4º × 10º split-beam transducer, operating in kHz frequency range, produces an elliptical acoustic footprint of respective major and minor axes of 1.7 m and 0.7 m at 10-m range, which can insonify the entire fish but provides no spatial resolution in either the major- or minor-axis direction. The resulting target information consists of only a few peak echoes from the major scattering organs such as the swim bladder, the head and/or the tail. It is difficult for users to visually relate these echoes to the original shape of the fish. Figure 11 schematically illustrates the difference in sonic views of a fish by regular and DIDSON sonars.

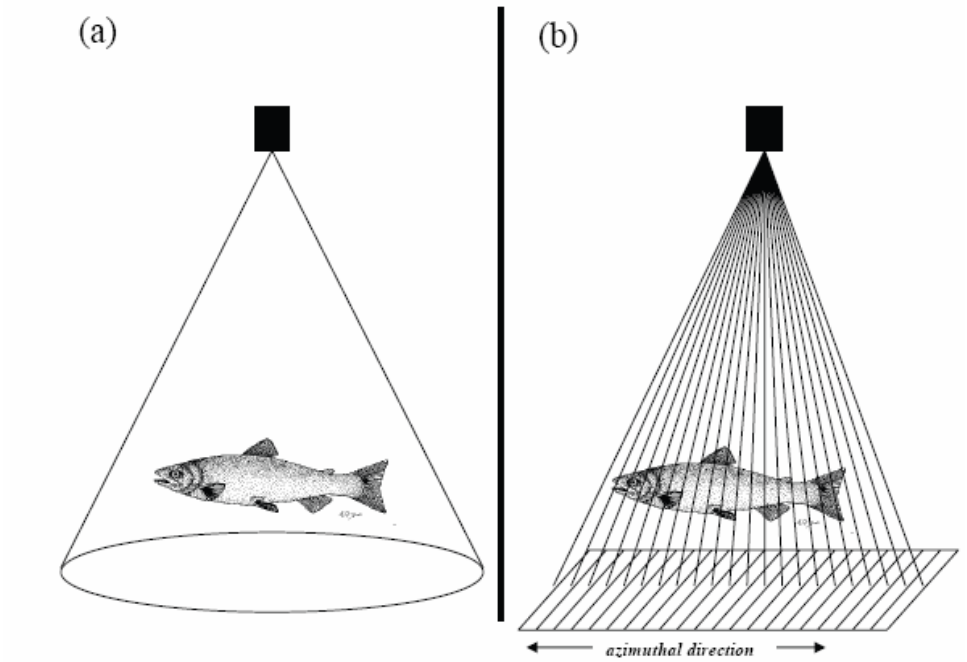

Fig. 5. Sonic views of a fish by (a) a regular sonar beam which provides no lateral resolution, and (b) by a DIDSON sonar beam that provides a sharp azimuthal resolution revealing the shape and body structure along the azimuthal direction of the beam.

During two field surveys in the early and late summer of 2007, a Standard DIDSON system and a Long-Range DIDSON system were deployed from our small aluminum boat (Fig. 6) and a number of transects were made in the areas insonified by the tripod sonars, in an attempt to verify oceanic salmon targets.

Fig. 6. Twenty foot aluminum boat used for CTD casts and DIDSON measurements in the waters around Chatham Pt. during the summer of 2007.

MODELING OF ACOUSTIC PROPAGATION

To properly interpret horizontal, or sidescan, acoustic backscatter data at extended ranges it is important to have a reliable model for the sound propagation properties of the water column. The required parameters for such a model are: 1) the vertical and spatial characteristics of the sound-speed field, 2) the bathymetry of the area being insonified, and 3) the type of bottom. Data were collected at the site in support of the model as detailed in the following sections.

Sound speed profiles in southern Johnstone Strait

Sound speed profiles in the waters insonified by the sonar systems at Chatham Pt. were obtained from CCGS Vector in March 2007 and from a small 20' aluminum boat that was hauled to the site during several trips to Chatham Pt. during the summer of 2007 (Fig. 6). A Seabird CTD (Conductivity, Temperature, Depth) sensor was repeatedly used to obtain depth dependent temperature and salinity data used to calculate the water column sound speed profile.

Figure 7 show typical temperature and salinity profiles from the waters around Chatham Pt. These particular profiles where collected from CCGS Vector on March 14, 2007. However, data collected in July and August showed the same features. The variability observed in the data is due to the tide, with differences associated with different water masses moving in and out of the area. As the tidal current increases (Fig. 4(d)) the water masses become different, with colder less-salty water coming in from the south (Fig. 4(c)).

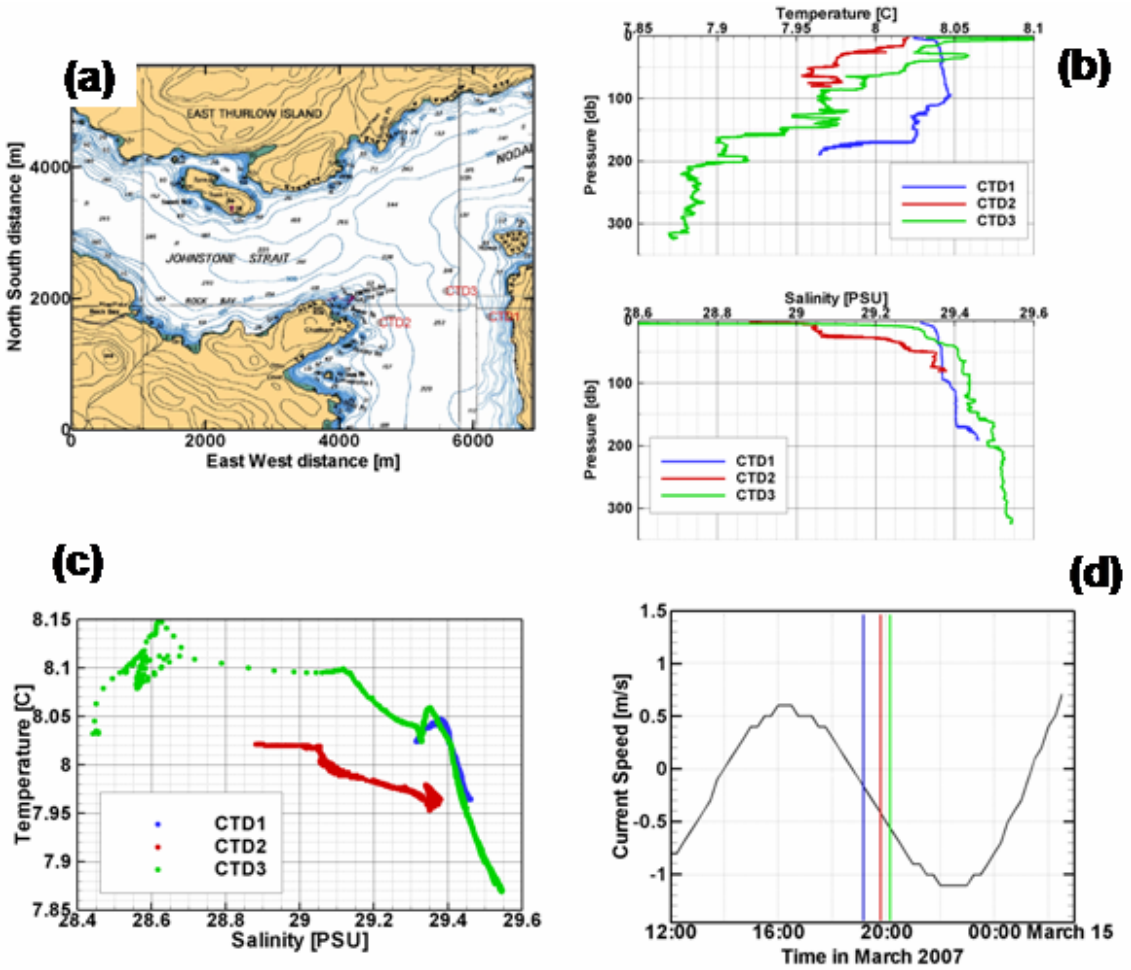

Fig. 7. CTD stations from March 14th 2007 at Chatham Pt. (a) shows the location of each of the 3 stations shown in (b-d). (b) Shows the temperature and salinity profiles from these stations and the Temperature versus Salinity plots in (c) show the differing water masses moving in. In (d) modeled current speeds are shown with the times of the three CTD profiles indicated. Negative values indicate ebbing, or north-flowing tide.

Currents at Chatham Point

It was not feasible during this study to obtain direct current observations at the site. We did deploy a small CTD on the tripod to measure the tidal elevation, but this instrument failed shortly after deployment. In subsequent further planned analysis of the collected data we will attempt to obtain tidal height information from the 100 kHz sonar system as we continue the analysis of the data collected during this study. However, this is a non-trivial task that will not be completed by the due date of this report.

For the analysis presented here we make use of the current model in the software program called "Tides and Currents" licensed to Fisheries and Oceans by Nautical Software Inc. From this software we find that the maximum current speed at Chatham Pt. during the study period was +/- 2.1 m/s. The current speed data from this software package had to be shifted by 5 hours to agree with our 100 kHz sidescan sonar data. This will be discussed in detail later in this report. An example of current speed data for a section of the tidal cycle is shown in Fig. 7(d), above.

Bathymetry

Bathymetric data for the area were obtained from the Canadian Hydrographic Service (CHS). Fortunately, the CHS had made a recent multi-beam survey of the waters around Chatham Pt (Fig, 8). From these data it is possible to extract a bathymetric profile along the main acoustic path of the 12 kHz sonar (displayed as the pie shaped figure starting from Chatham Pt. and going north in Fig. 8). The resulting bathymetry along this path is shown in Fig. 9. This depth versus range profile was subsequently used in the acoustic propagation modeling done for this study.

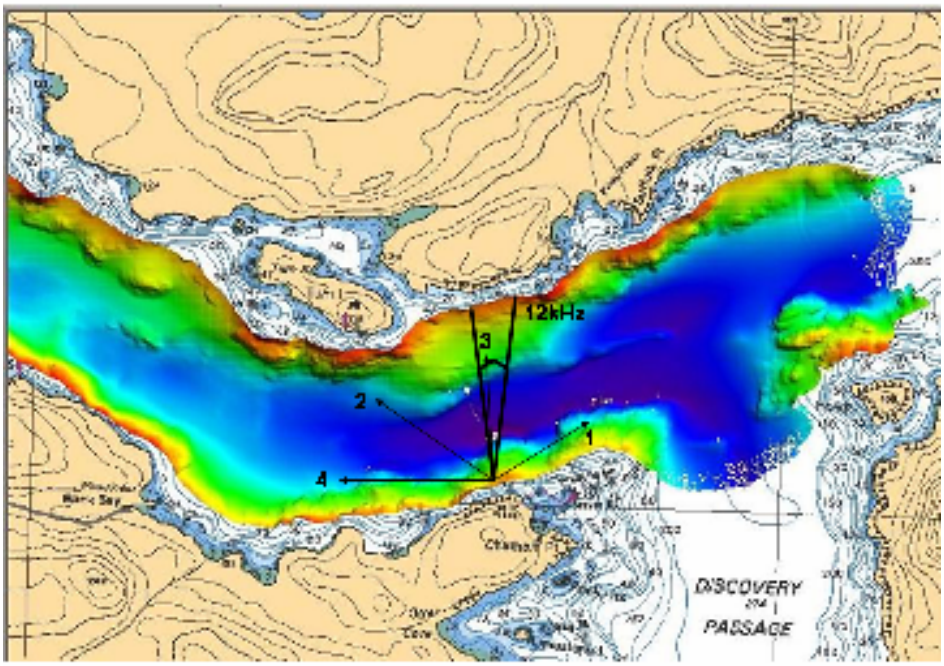

Fig. 8. Multi-beam data from CHS showing the bathymetry in southern Johnstone Strait. Dark blue in the center of the channel indicates depths exceeding 300m. The deep central part of the channel is clearly seen in the figure. Also shown are the directions of the different sonar beams from the tripod with the channel numbers indicated.

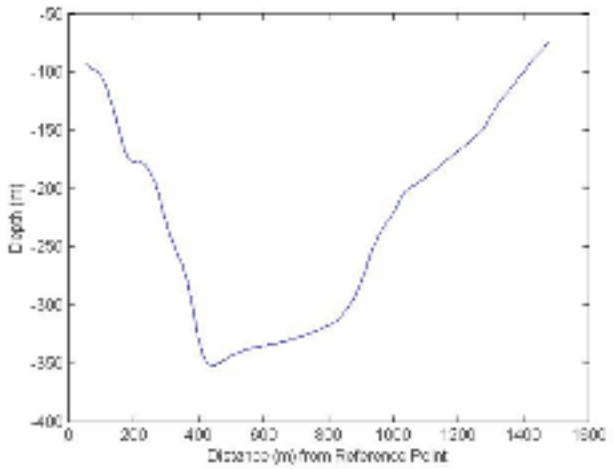

Fig. 9. Bathymetry along the path of the 12 kHz intermediate range sonar beam across Johnstone Strait from Chatham Pt. to East Thurlow Island.

Propagation modeling

The acoustic propagation conditions in the observation area are modified based on ray tracing code implemented by Bowlin et al. (1992). Sound pressure as a function of range and depth can be calculated using the code, given sound speed profile, sound source depth, and bathymetry. Figure 10 shows an example of eigenray paths across the channel, for the given sound speed profile (red line) and bottom profile (blue line). In this example, we assume that the sound speed is horizontally homogeneous.

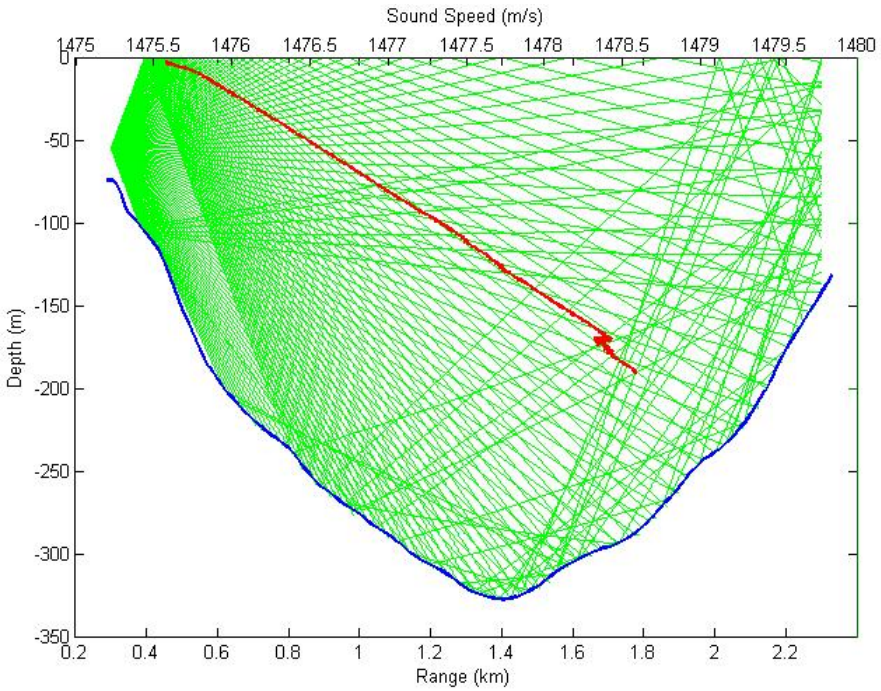

Fig. 10. Eigen ray paths across the channel. Blue line is the bottom profile and Red line is a sound speed profile from Chatham Point. Note that the scale difference in x (~2000m) and y (~350m) causes the apparent angles of ray direction to be distorted.

Figure 11 shows acoustic intensity distribution in the field under the same conditions as in Fig. 10. Bottom reflections in the forward direction are modeled by a classical two-layer model, but the reflections in the opposite direction of propagation are not included (limited by the ray tracing code). Absorption is also not included, but is not expected to be important at 12 kHz and within the range. Vertical beam angle ranges from -30 deg to 30 deg, and it is assumed that the beam is uniform within these angles. The software package (MASTER) provides a user-interface for running the ray-tracing code, by allowing the user to load sound speed profiles and bottom profiles and set a number of other parameters. It is clear from the simulations that in well mixed waters like experienced at Chatham Pt. and with the presence of surface reflections, most of the water column will be insonified by the sonar beam.

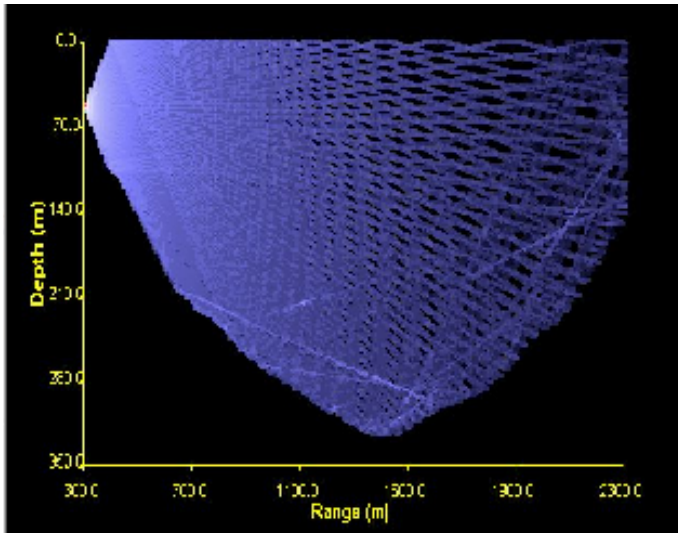

Fig. 11. The acoustic backscatter intensity distribution. Vertical beam angles range from -30 deg to 30 deg. Bottom reflections in the opposite direction of propagation are not included (limited by the ray tracing code). Absorption is not included, but is not expected to be important at 12 kHz within the range. The sonar array beam pattern is not included. As can be seen, most of the water column will be insonified.

SIGNAL PROCESSING AND TARGET DETECTION FOR 12 KHZ SONAR SYSTEM

Pattern recognition algorithms for target tracking

A key technical issue in this project is to estimate fish passage across the sonar beam. Estimation of fish passage can be performed either by tracking individual targets or by applying echo integration to a sampling volume. Multiple-target tracking (MTT) has been a classical problem in radar and sonar surveillance (Blackman and Popoli, 1999). It originated from radar tracking of aircraft, but has also been encountered in many underwater applications, such as passive tracking of breaking ocean waves with a hydrophone array (Ding and Farmer, 1992) and split sonar tracking of fish (Xie, 1999). Echo integration has been extensively applied to fish abundance estimation in marine environments over the past decades, with success varying in different conditions (Simonds and Maclennan, 2005; Medwin and Clay, 1998).

Before the start of this project, we had developed a preliminary target-tracking algorithm (based on echograms) for the 12 kHz sonar data obtained earlier in Georgia Strait (Farmer et al., 1999). Figure 12 shows an echogram from the Georgia Strait data, where the white traces are likely due to fish, and the red dots represent echo traces picked up by the tracking algorithm. The sonar transmitted a linear FM sweep from 11.2 to 12.8 kHz, increasing range resolution substantially. The data in Fig. 12 had a range resolution better than 0.5m.

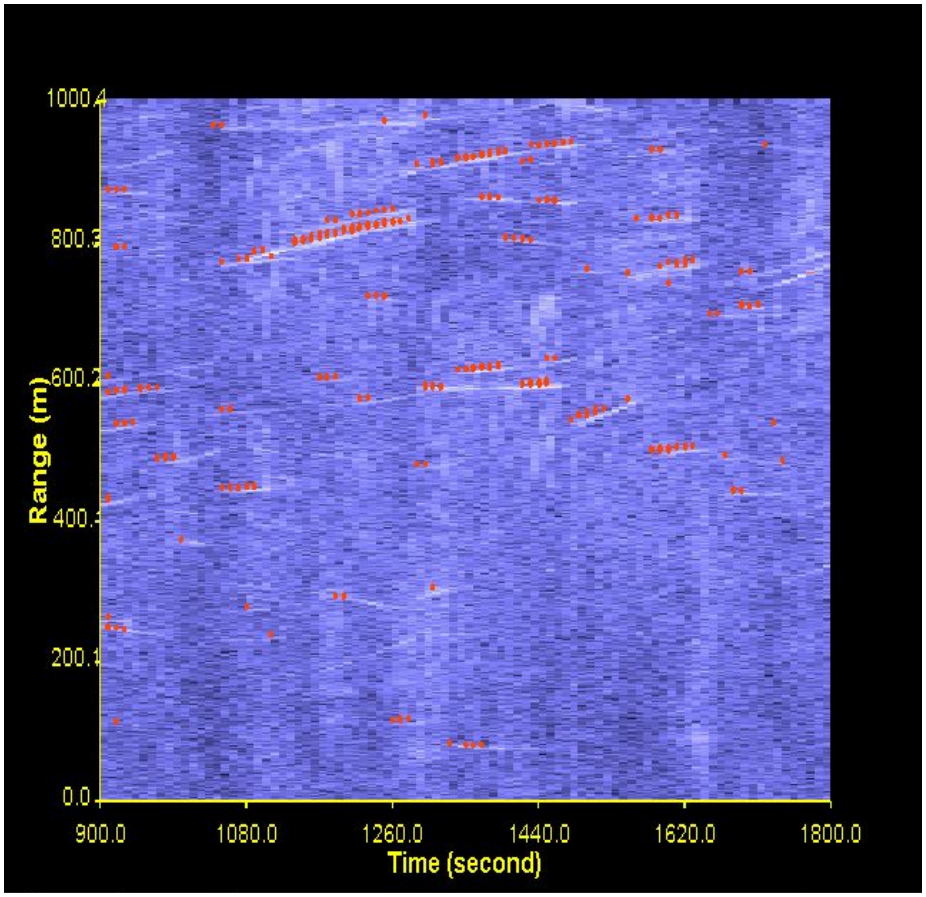

Fig. 12. Echogram from the 1999 Georgia Strait data, where the thin white streaks are likely to be associated with single fish. The red dots represent the data identified as fish traces by the tracking algorithm.

A new challenge in this project is that the 12kHz sonar did not operate at the FM sweep transmission as it had done before, due to environmental concerns. Figure 13 shows an echogram from the data collected at Chatham Pt. The range resolution was reduced to around 2m, and the echo traces appear to extend much wider in range than those in Fig. 12. Therefore, while it is possible that each trace in Fig. 12 is associated with a single fish, we can no longer assume that the echo traces in Fig. 13 are associated with single fish.

Therefore, a logical way of estimating fish passage in this project was to take a hybrid approach. It is still necessary to isolate individual echo traces such as those in Fig. 13 and the required algorithm would be similar to the one used to track individual traces in Fig. 12. However, instead of counting each cluster of traces as a single fish, echo integration can be used to the regions covered by the isolated clusters of echo traces. Even though the echo integration approach was developed for the data collected during this study, the lack of accurate system calibrations made it impossible to implement the technique at this stage. As a result, the results presented here only make use of the sonar raw data,

The tracking algorithm is discussed here while the theoretical basis of the echo integration approach has been left to the Appendix.

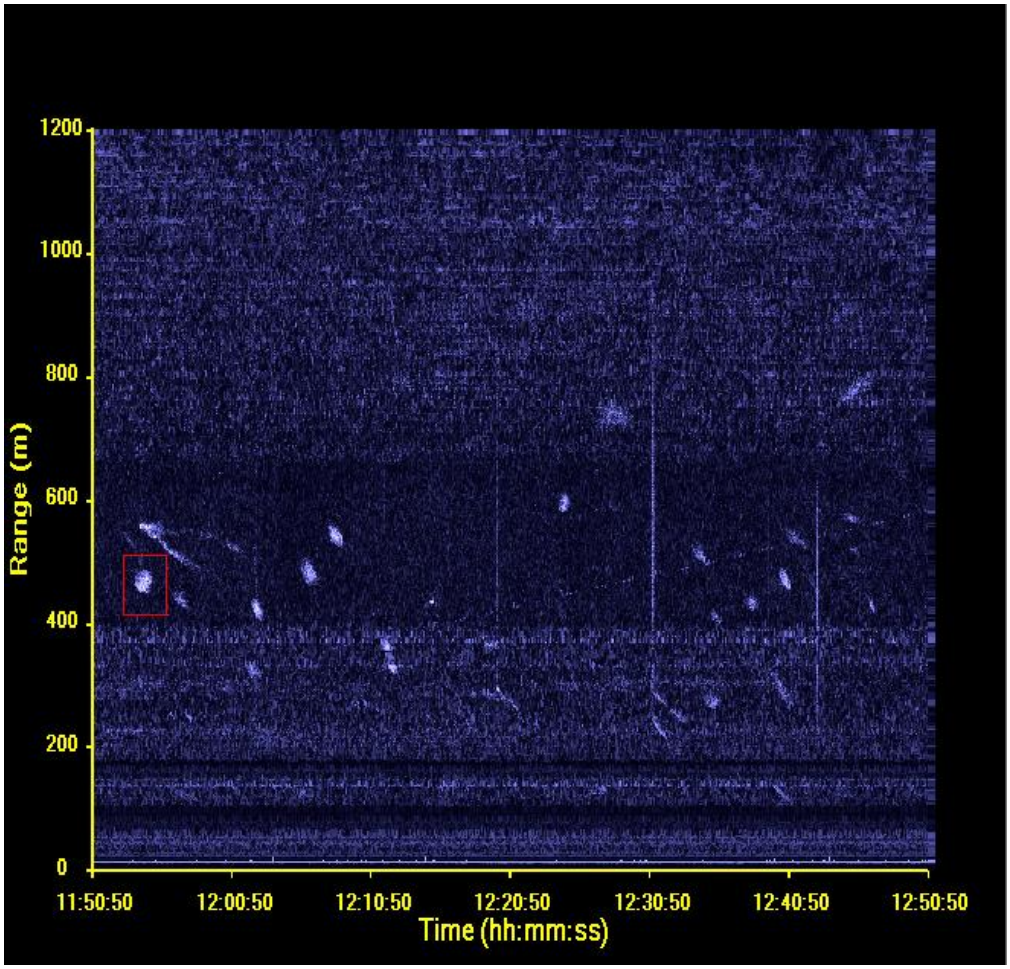

Fig. 13. Echogram from the 2007 Chatham point data, where the white clusters such as the one in the red box are likely to be associated with multiple fish.

The tracking algorithm is based on cluster analysis of objects on images (such as the echograms in Figs. 12 and 13). As in typical pattern recognition problems, preprocessing of the image is a crucial step towards success. In Fig. 13, for example, the background reverberation has been removed from the raw data. There is some interference leading to observable vertical stripes. While the interference can be eliminated with a 2D filter, some data associated with the target traces will also be eliminated. Unless strong interference exists it is best to avoid the use of filtering. However, if the image appears too noisy, a smoothing filter will be used to suppress random noise. With the background noise suppressed and the reverberant interference removed, a threshold can effectively be used to select a subset of the data with echo intensity above a selected threshold. Following these steps cluster analysis is applied to the output to sort the selected data into individual clusters for further analysis.

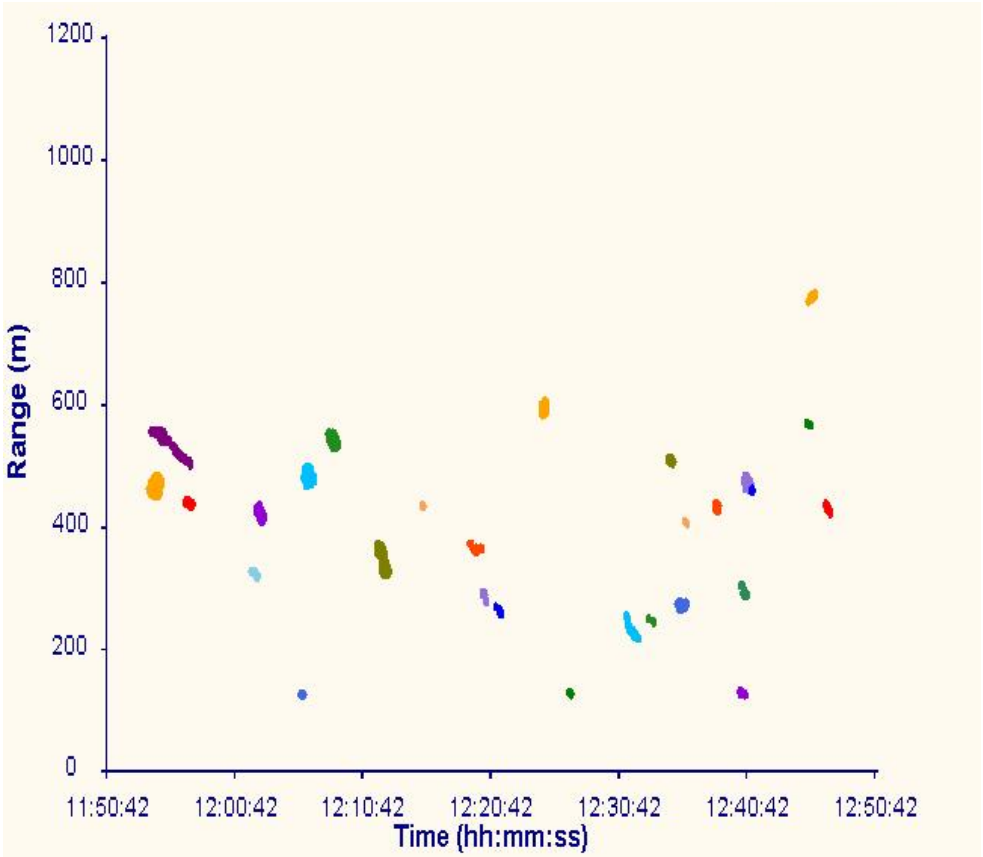

Fig. 14: The clusters in Fig. 13 are identified as fish traces by the tracking algorithm. Colors represent different traces.

Cluster analysis is a process of partitioning a set of objects into groups, or clusters, in such a way that objects in the same cluster are very similar by some measure and those in different clusters are significantly different. Cluster analysis of images has been used to isolate and track numerically simulated breaking ocean surface waves (Ding, 1993). In this project, a hierarchical clustering algorithm was used (Theodoridis and Koutroumbas, 2003). This algorithm first treats each object as a cluster and then joins the two closest, or most 'similar', objects to form a cluster. The two closest clusters from the remaining objects (each treated as a cluster) and the first-formed cluster, are merged to form a new cluster, which joins the other clusters to form another new cluster, and so on. The algorithm proceeds until the selected criterion is satisfied, or until all the objects collapse into a single cluster.

There are two thresholds required in our cluster analysis. The first one is an echo intensity threshold. This is typically dictated by the signal-to-noise ratio in the image data. The second one defines the minimum distance between clusters before they are joined to form a larger cluster. These thresholds can be determined initially by trial and error, but once typical values for the data are found, a statistical approach can be used. The clustering result is more sensitive to the intensity threshold, which needs to be determined first. One approach is to calculate the total number of clusters in a given period, for varying thresholds. The number of clusters should initially decrease rapidly with increasing intensity threshold, but the decrease should slow down as the intensity threshold continues to increase. Therefore, we chose a typical intensity threshold at which the change of the number of clusters is smallest. We then fixed the intensity threshold and varied the distance threshold to examine the dependence of clustering results on the distance threshold.

As the distance threshold increases, we expect fewer clusters to remain. Visual inspection of the clustering results aided in determining the effective distance threshold.

Figure 14 shows the extracted echo traces from the data in Fig. 13, with the colors representing different traces. These extracted trace data define the temporal and spatial span of each trace. In the next section, we will discuss the issue of how to estimate fish passage associated with each individual trace.

The tracking and display tools have been implemented in a software package named MASTER (Marine Acoustics Solution Tools for Experimental Research), which also includes modeling of acoustic propagation.

TARGET DETECTION FOR 4-CHANNEL 100 KHZ SIDESCAN SONAR SYSTEM

The processing of the 100 kHz sidescan sonar data followed a much simpler and less sophisticated procedure than the technique used for the 12 kHz intermediate sonar system as outlined in the previous sections. The 100 kHz sonar system was included because it already was available, to investigate whether such a system may be used to detect migrating salmon closer to shore (~100 m). It quickly became apparent that this system was much more prone to masking by turbulent tidal mixing of bubbles in the upper ocean and by wakes from boats and ships.

Target detection

The raw backscatter intensity data from each of the 4 channels were averaged over each file, typically 7 minutes, and the resulting average was subtracted from the original data in a given file. This procedure served two purposes: 1) To compensate for spreading losses in the channel, and 2) to remove signals from stationary targets, such as rocks or other bottom features. Some examples of the resulting 'corrected' backscatter data are shown in Figures 15-17. Figure 15 shows the effect of strong tidal mixing on the upstream and downstream channels (Channels 4 and 1 in Fig. 8) during flooding. Bubbles generated by the tide are being swept towards the upstream transducer resulting in long downward tilted streaks of high backscatter. The reverse is true for the downstream channel where the bubble plumes are being advected away from the transducer, resulting in streaks or bands tilted upwards. These features will be discussed further below.

Figure 16(a) is an example of observed backscatter from a pod of Orca whales moving through the area. The observed strong targets correspond directly to times when the lighthouse keepers noted the presence of a killer whale pod near the tripod. Figure 16(b) is a typical example of the acoustic signature of a large vessel passing the instrumentation. The direct active noise signal from the cavitating propeller, showing up as a vertical line in the spectrogram, is immediately followed by the backscatter data from the bow and stern wakes of the vessel. This type of target is very common in our data, especially during periods near slack tide, which obviously is the preferred time for any large vessels to travel through the channel.

Finally, Fig. 17 is an example of 100 kHz backscatter intensity from fish targets, which are the targets of interest in this study.

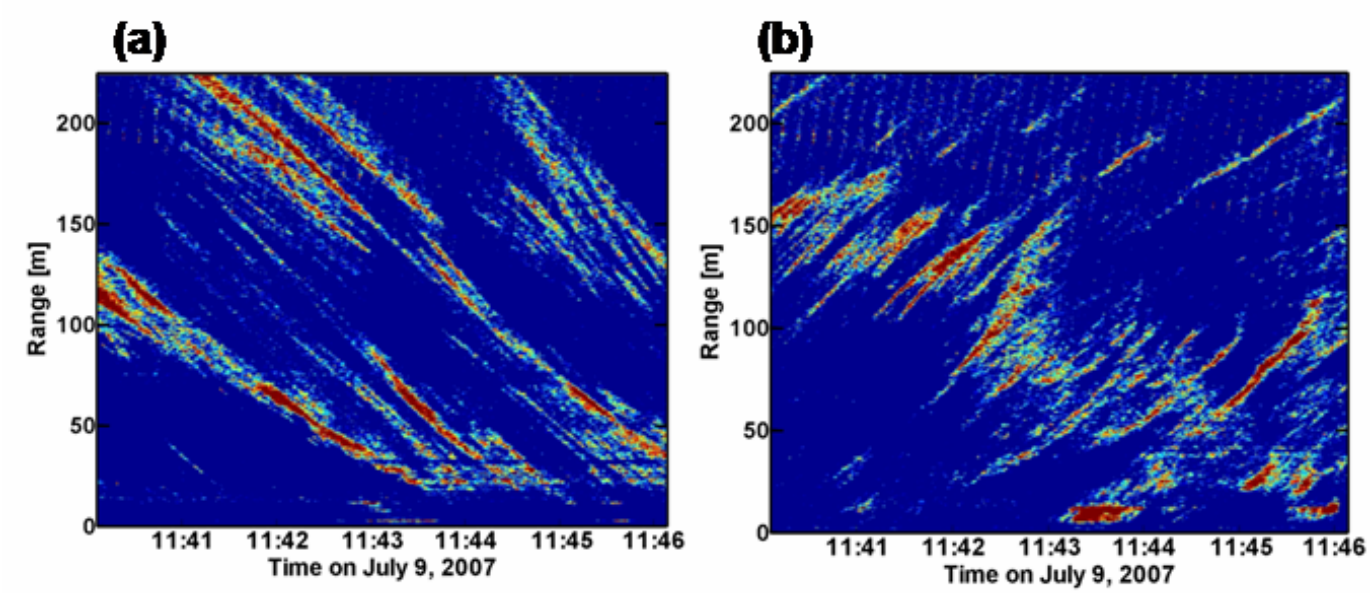

Fig. 15. Typical example of 100 kHz sidescan sonar data during strong flooding tide. (a) Shows the backscatter data from Channel 4 which is the upstream sonar (Fig. 8). The bubble plumes generated by the tidal turbulence moves towards the transducer. (b) Is the corresponding Channel 1 (Fig. 8) data where the bubble plumes are advected away from the transducer and down the main channel. (Red indicates strong backscatter and blue indicates weak or absence of backscatter).

The procedure used to detect targets in data of the type shown in Figures 15-17 consisted of searching for sections in the data where pixels next to each other where all above a certain threshold level, in a similar fashion to the procedure used on the 12 kHz array data. Only targets that consisted of more than 100 pixels were kept to minimize the effect of electrical and acoustical noise. Figure 18 shows an example the procedure. For each of the detected targets information about time, mean range, target size, shape of the target, and the backscatter intensity of the target were stored in a new file for further processing. The shape of the target gives a measure of whether the target has elongated shape like the bubble plumes in Fig. 15 or a more symmetrical shape like the fish targets in Fig. 17. For the elongated targets we also recorded their orientation. In the subsequent discussion we are assuming that the target counts generated from the 100 kHz sonar data represent individual fish. This is probably not a bad assumption since the range bins of this system was 0.37 m and with one transmission, or ping, every 0.5 second.

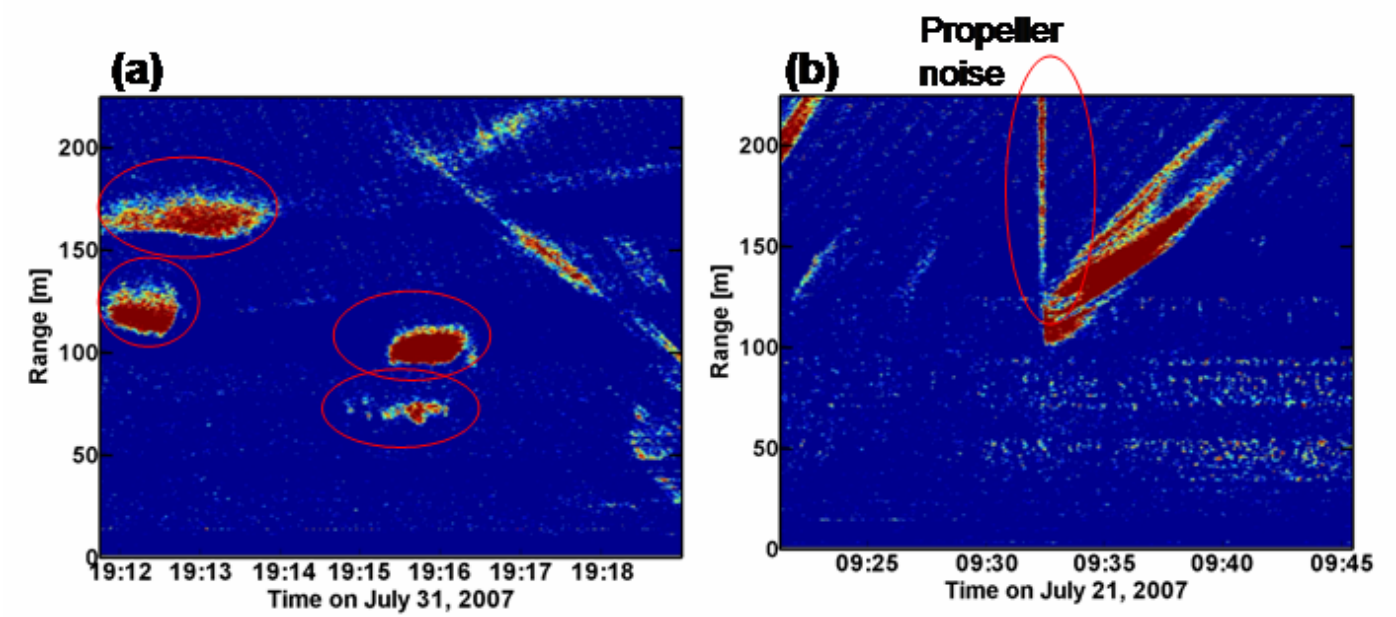

Fig. 16. (a) This is a 100 kHz backscatter example of probable backscatter signal from Orca whales moving through the area as reported by the lighthouse keepers at this time. (b) Typical example of a larger vessel, tug or cruise ship, moving through the sonar beam. The vertical line shown inside the ellipse is direct noise from the ship reaching the transducer, followed by the bow and stern wakes.

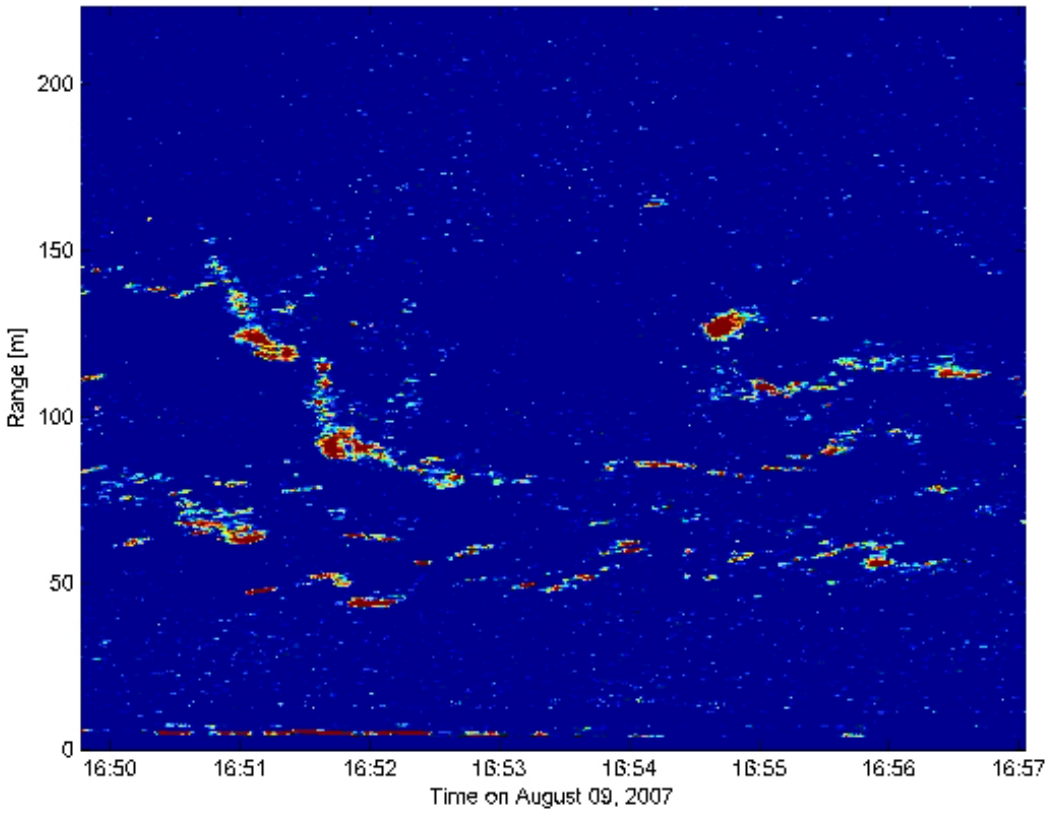

Fig. 17. An typical backscatter example of fish passing within 150 m of channel 2(Fig. 8) 100kHz transducer.

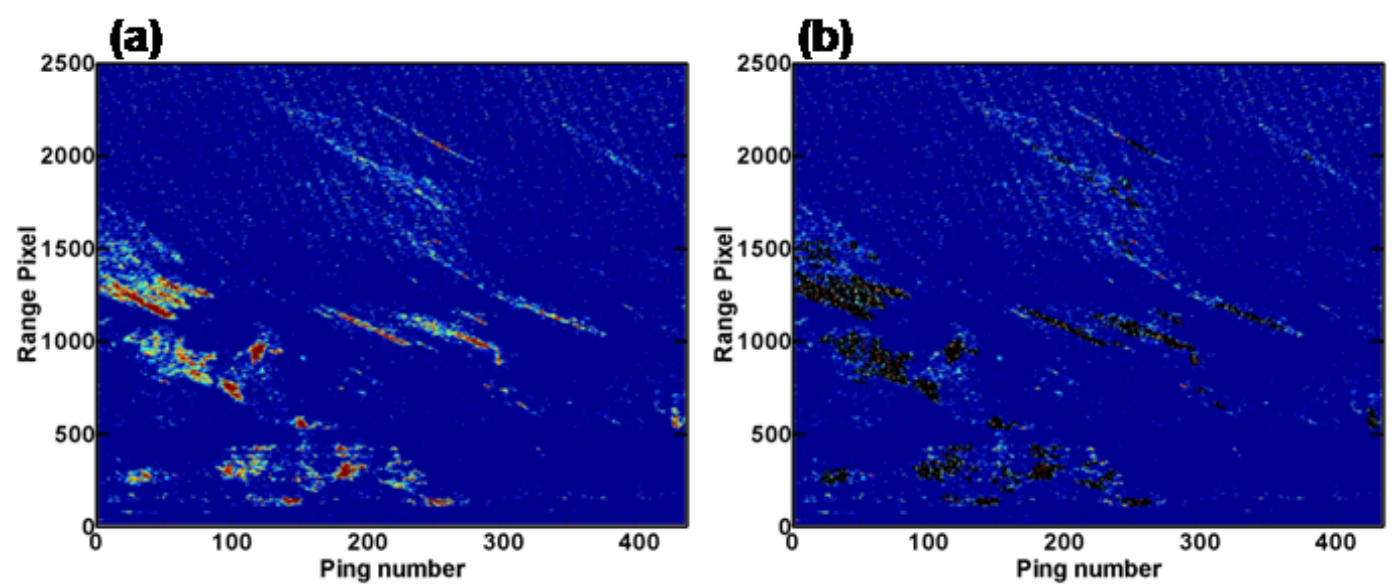

Fig. 18. (a) An example of backscatter intensity data from Channel 1 (100 kHz) for a 400 second period, and (b) the same data with the detected targets shown in black.

Fish targets were classified as targets at ranges between 20 and 250 m that consisted of between 100 and 500 pixels. Investigations found that this excluded most of the elongated targets associated with tidally generated bubble plumes and the larger targets associated with boat and ship wakes.

Target orientation and tidal current

It is obvious from Fig. 15 that the long thin tilted targets associated with bubble plumes being advected with the tidal current, will be related to the strength and direction of the tidal flow. In Fig. 19 the orientation of all detected targets consisting of more than 10,000 pixels (i.e., large targets) has been plotted for the upstream and downstream (Channels 4 and 1, Fig. 8) sonars for a six day period in July. (The plotted orientation is relative to the time and range scales of the system).

Several interesting features can be seen from these data. One puzzling feature is that to get agreement between the modeled current speeds and the target observation the current data have to be shifted by 5 hours. It is also interesting to see that most of the generation of these large elongated targets happens during the flood, or southward flowing, part of the tide. There seem to be an asymmetry in the bubble generating properties of the tidal flow around Chatham Pt that we presently can not explain. Nevertheless, it is clear that the unique acoustical signatures observed during flooding (south flowing) tide can be utilized to differentiate non-fish targets from fish targets and therefore let us minimize target recognition biases in the resulting fish track data. This is fortunate since it is during flooding tides that most of the migrating salmon will pass the sonar system.

However, there is an exception to this asymmetry on July 9th when significant numbers of targets were detected during both cycles of the tide. The opposite orientation, and therefore possibly the direction of travel, of the targets detected by the two opposing sonars is clear from these data. A closer examination of the data is required to explain these processes.

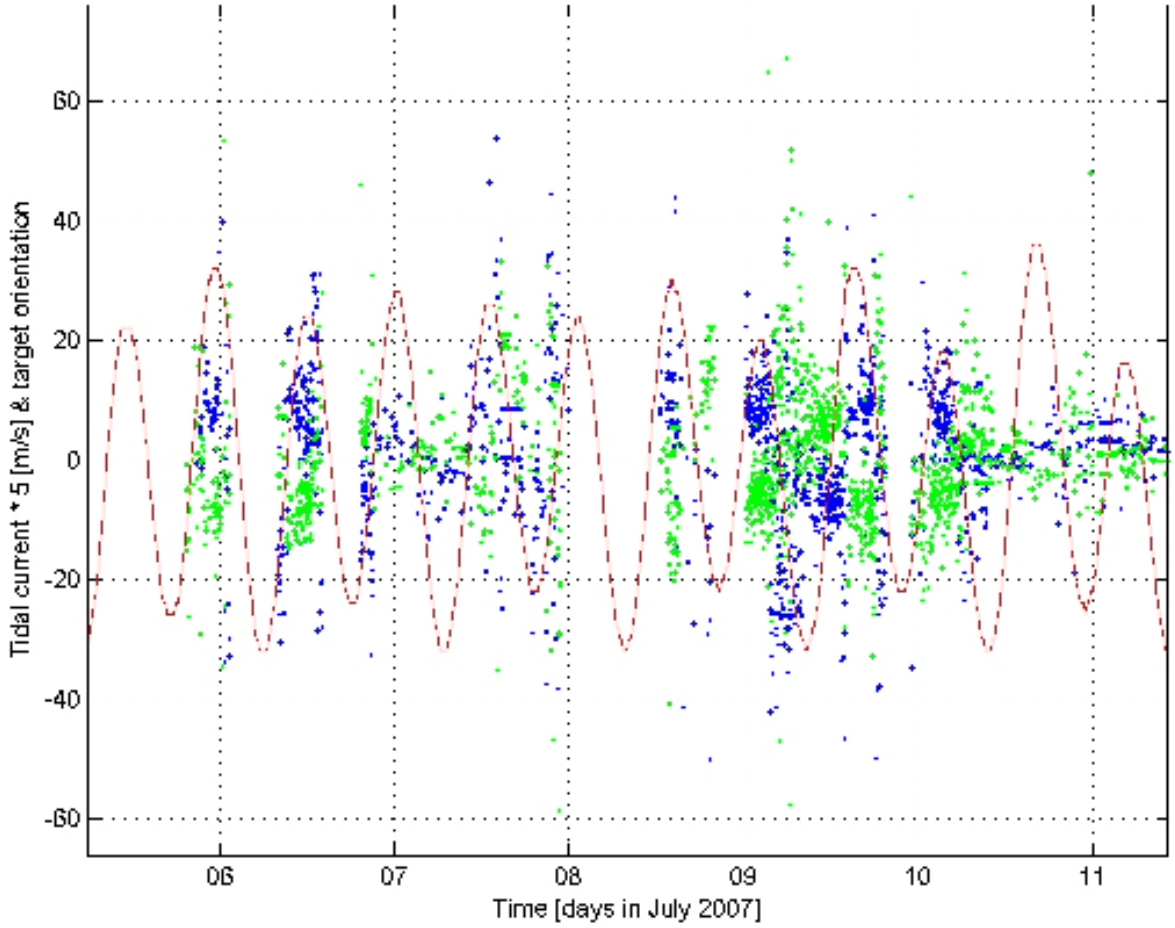

Fig. 19. Tidal current in m/s scaled by 5 (red line) and orientation of large backscatter targets from channel 4 (green dots) and channel 1 (blue dots) for a six day period in July when data were available. The current data have been shifted by 5 hours to correspond with the sonar observations.

RESULTS

Information about number of detected targets per unit time detected with the two sonar systems using the approaches outlined above can now be compared to each other and related to the very limited available test fishery data and to the fish count estimates from the fish counts at Mission.

It is worth noting that the 2007 season was extremely poor for the number of returning sockeye salmon to the Fraser River system, resulting in low numbers of acoustical targets to work with at Chatham Pt. and

increased statistical uncertainties in the test fishery estimates. The result may be that 2007 ended up being a less desirable year for this type of comparison.

Target counts from 12 kHz intermediate range sonar and 100 kHz sidescan sonar system

Using the target detection techniques discussed in earlier sections it was possible to come up with daily estimates of number of detected fish-like targets for the two sonar systems. These results from July 20th and into September are shown in Figure 20. The number of target clusters detected by the 12 kHz sonar have been inflated by a factor of 50 in the figure, which suggests that the targets detected by this wider beam and larger range bin size sonar system actually consists of schools of fish with each school comprising several individual fish swimming together. Further, planned processing of the data in which sonar calibrations and estimated target strengths of individual fish are included should be able to determine the actual value of this scaling factor. In this report we will use a value of 50 in our comparisons with independent available data.

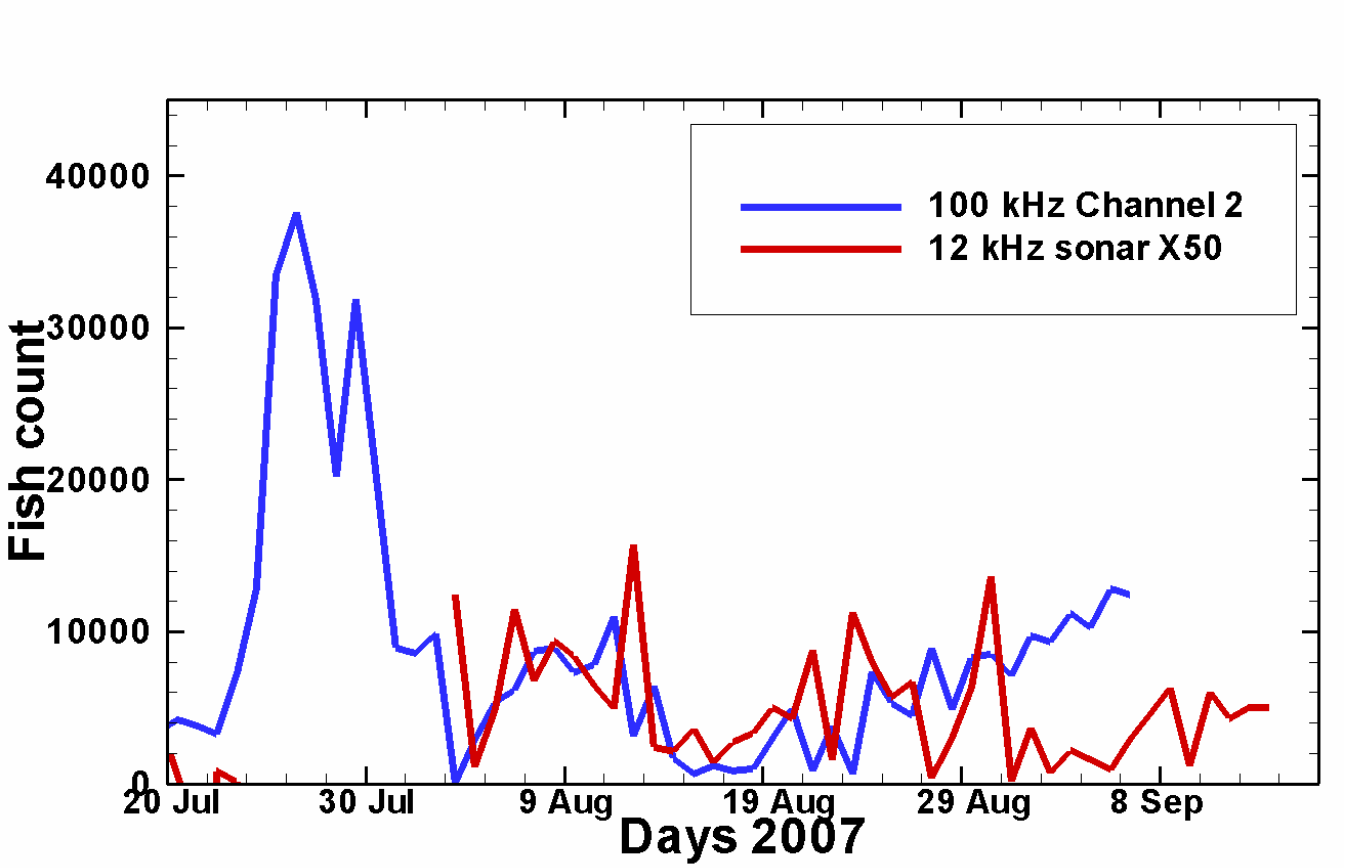

Fig. 20. Estimates of total number of targets detected per 24h period from the 12 kHz sonar (red) and the channel 2 (Fig. 8) 100 kHz sidescan sonar (blue). Please note that the 12 kHz data have been scaled by a factor of 50 in this figure and the figures to follow.

Unfortunately, an operator error on July 24, where the 12 kHz sonar transceiver was remotely put into a continuously transmitting mode, which damaged the transmit transistors, and rendered the system inoperable from July 24th to August 4th. On August 4th we returned to Chatham Pt. and replaced the transistors. This is a clear example of Murphy's Law in action, since as can be seen in Fig. 20 this period

turned out to be the main sockeye migration period for this area. Fortunately the 100 kHz system was working throughout this period and the results plotted in Fig. 20 show a large pulse of targets, presumably sockeye salmon, moving through the area during the period from July 24th to August 2nd. By using the scaling of 50 for the 12 kHz sonar system we see good agreement between the two systems, including a second peak in the number of targets between August 4th and August 12th. However, in late August the two target estimates start diverging suggesting changes in the target composition, with the 12 kHz estimates staying low while the 100 kHz estimates increasing. A possible explanation for this is that pink salmon showing up in the latter parts of August may travel closer to shore and therefore are not detectable by the 12 kHz sonar. This possibility will be discussed further in a later section.

Acoustical fish counts and Areas 12 and 13 test fishing results

For parts of the measurement period at Chatham Pt. the Pacific Salmon Commission did purse seine and gillnet test fishing at different locations around Vancouver Island (Fig. 21). Areas 12 and 13 in Johnstone Strait were the locations closest to our Chatham Pt. measurement site with Area 13 being the nearest. However, due to funding constraints, test fishing information from Area 13 is unavailable for July.

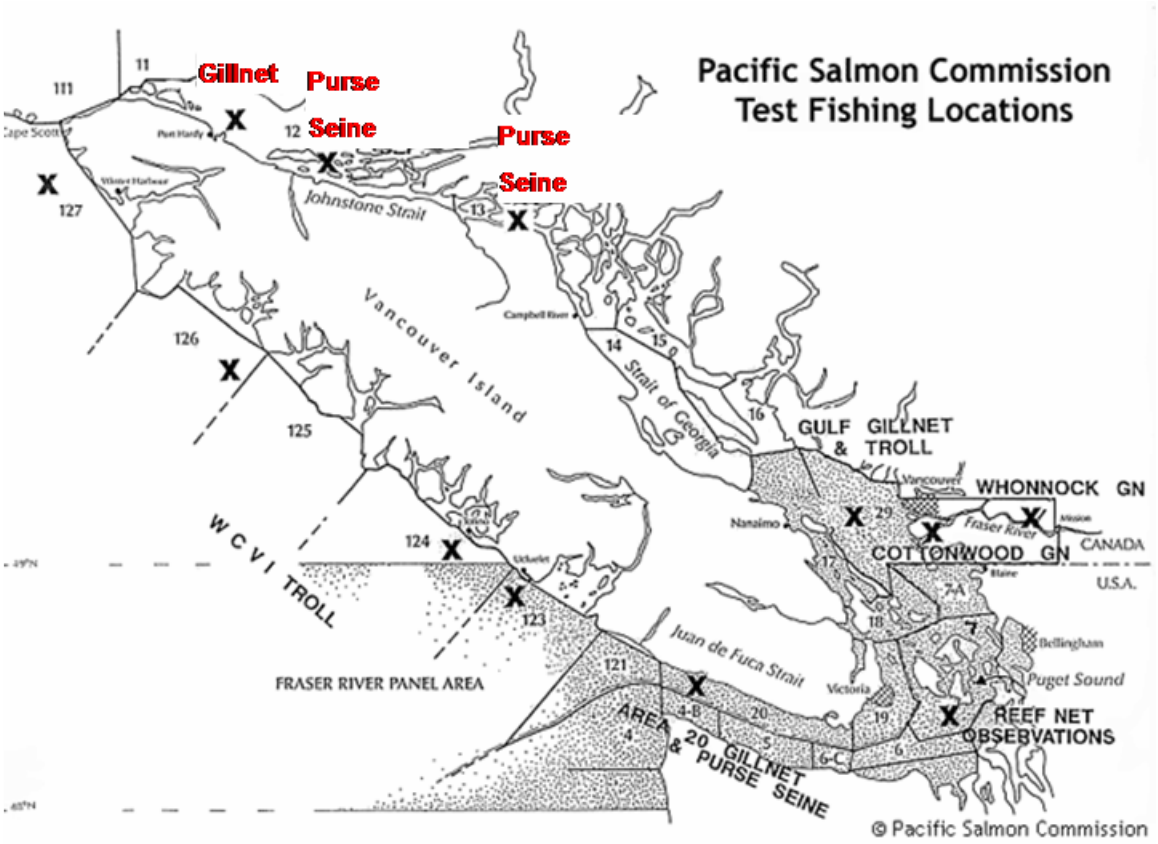

Fig. 21. Pacific Salmon Commission Test Fishing Locations. Areas 13 and 12 in Johnstone Strait are the areas closest to our measurements at Chatham Pt.

The fish count, or number of detected targets per 24 h period, detected acoustically have been plotted with the test fishery catches in Fig. 22. It is worth noting that that test fishery catches during this period was exceptionally low for this area.

It is difficult to find any strong correlation between these two data sets except for perhaps a correlation between the sockeye test-fishery catches between August 5 and August 19 and the broad peak in the acoustically detected targets during parts of the same period. A similar relationship can perhaps be seen for pink salmon between August 19th and August 29th (Fig. 22, lower panel).

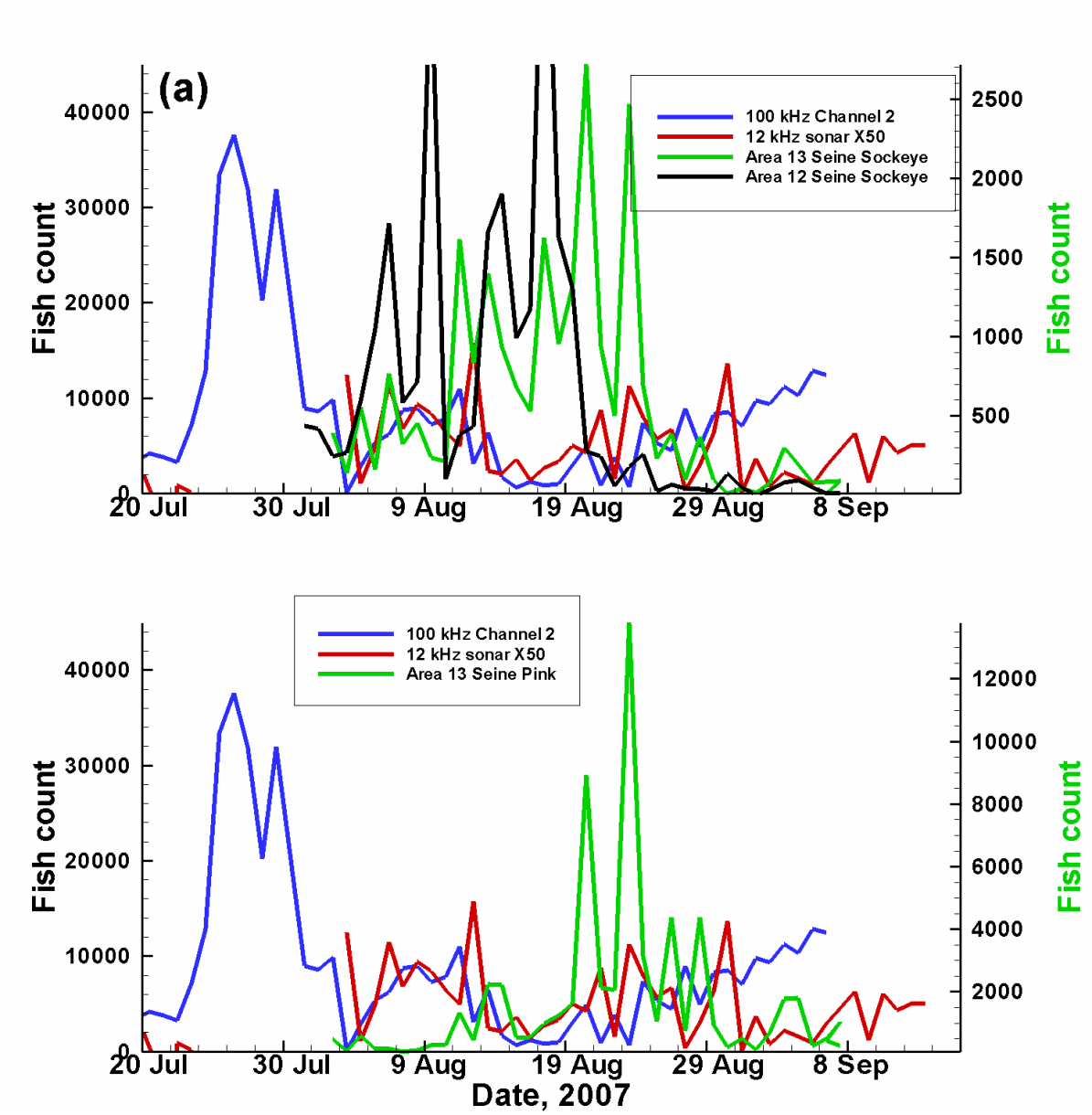

Fig. 22. Chatham Pt. acoustically detected fish targets (blue and red lines) plotted with Seine test fishery catch estimates with Area 13 estimates in green and Area 12 estimates in black. The upper figure shows the test fishery data for sockeye salmon and the bottom figure show the corresponding catches of pink salmon. The acoustically detected fish counts are on the left y-axis while the test fishery estimates are on the right y-axis.

Acoustical fish counts and Fraser River Mission counts

The results from the Chatham Pt. acoustical fish detection system can also be compared to the in-season fish counts from Mission, in the Fraser River. In Fig. 23 the acoustically detected daily target, or fish, counts obtained at Chatham Pt. have been plotted with the Mission estimates for both sockeye and pink salmon, and in Fig. 24 the same data have been plotted except for the Mission estimates being shifted by 9 days. Several interesting observations about the sockeye salmon fish estimates can be extracted from the data shown in these figures;

1. The 100 kHz fish counts at Chatham Pt. are half of the overall Mission counts throughout the sampling period. Here it is important to remember that the Mission counts include fish arriving from both the northern approach via Johnstone Strait **and** the southern approach through Juan de Fuca Strait.
2. The estimates are separated in time by approximately 9 days. In other words, the sockeye salmon showed up at Mission 9 days after they passed Chatham Pt.
3. The peak at Chatham Pt. is narrower than the peak at Mission. There are at lease two hypotheses that may explain the widening of the arriving pulse observed at Mission. One is that after the fish pass Chatham Pt. they spread out into Georgia Strait and spread their arrival time into the Fraser River out over a longer time period; the other is that the pulse past Chatham Pt. amalgamated with fish pulses arriving a few days later from Juan de Fuca Strait to form a much more protracted pulse of in-river flux at Mission.
4. The second peak in the sockeye estimates observed at around August 22 (Fig. 23) at Mission may be related to the peak observed around August 10 at Chatham Pt.

There is no direct comparison for the pink salmon peak observed at Mission in early September due to shutdown of the Mission site.

To refine this comparison we need to look closer at a reconstructed run size for Area 13 from Mission data plus divergent rate and delays, including the fact that Area 13 fish take approximately 2 more days than Area 20 (Juan de Fuca) fish to arrive at Mission.

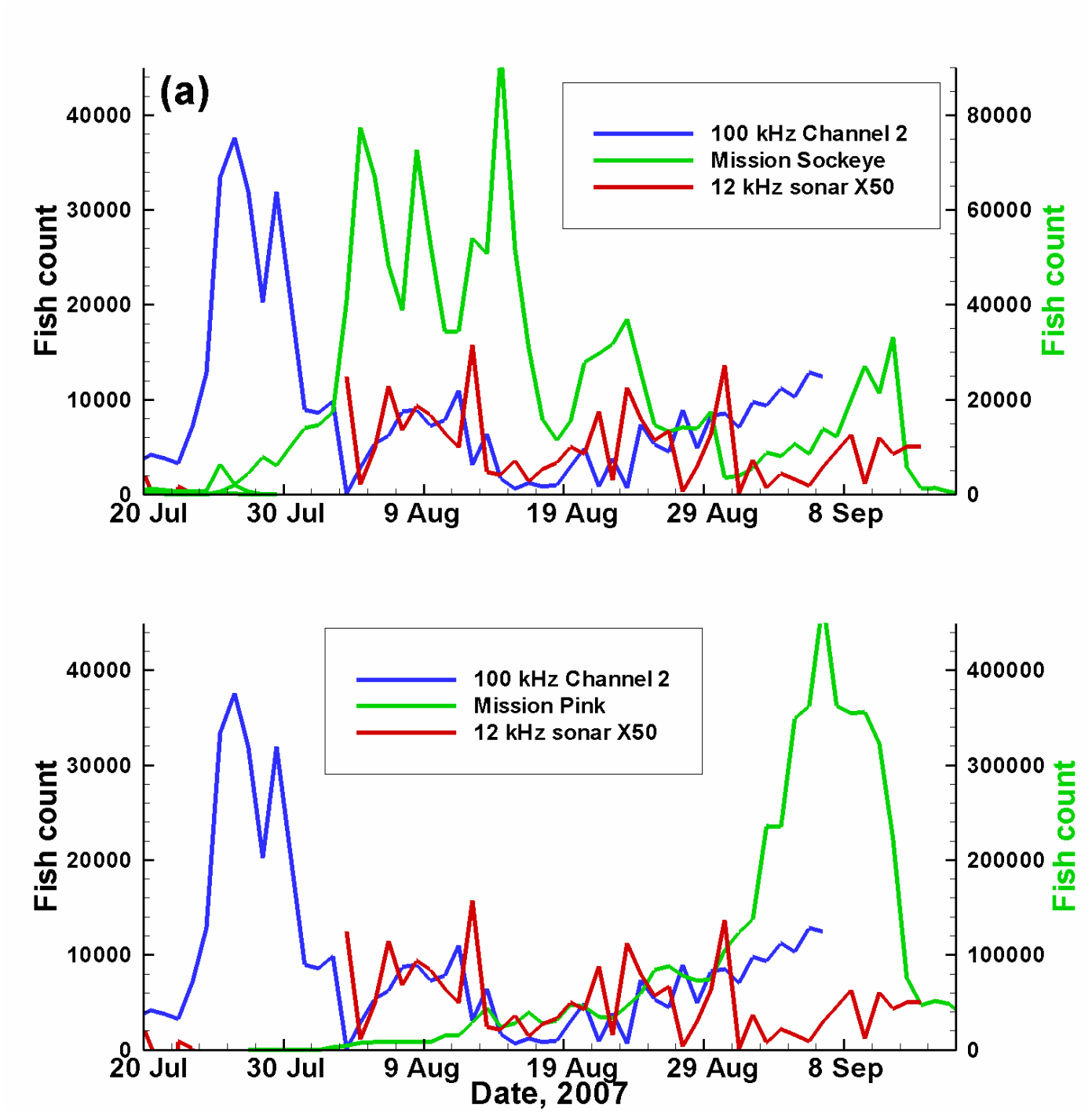

Fig. 23. Chatham Pt. acoustically detected fish targets (blue and red lines) plotted with Mission estimates (green line). The upper figure shows the Chatham Pt. data and the sockeye salmon counts from Mission and the bottom figure shows the corresponding pink salmon Mission estimates. The Chatham Pt. data are using the left y-axis while the Mission estimates are using the right y-axis.

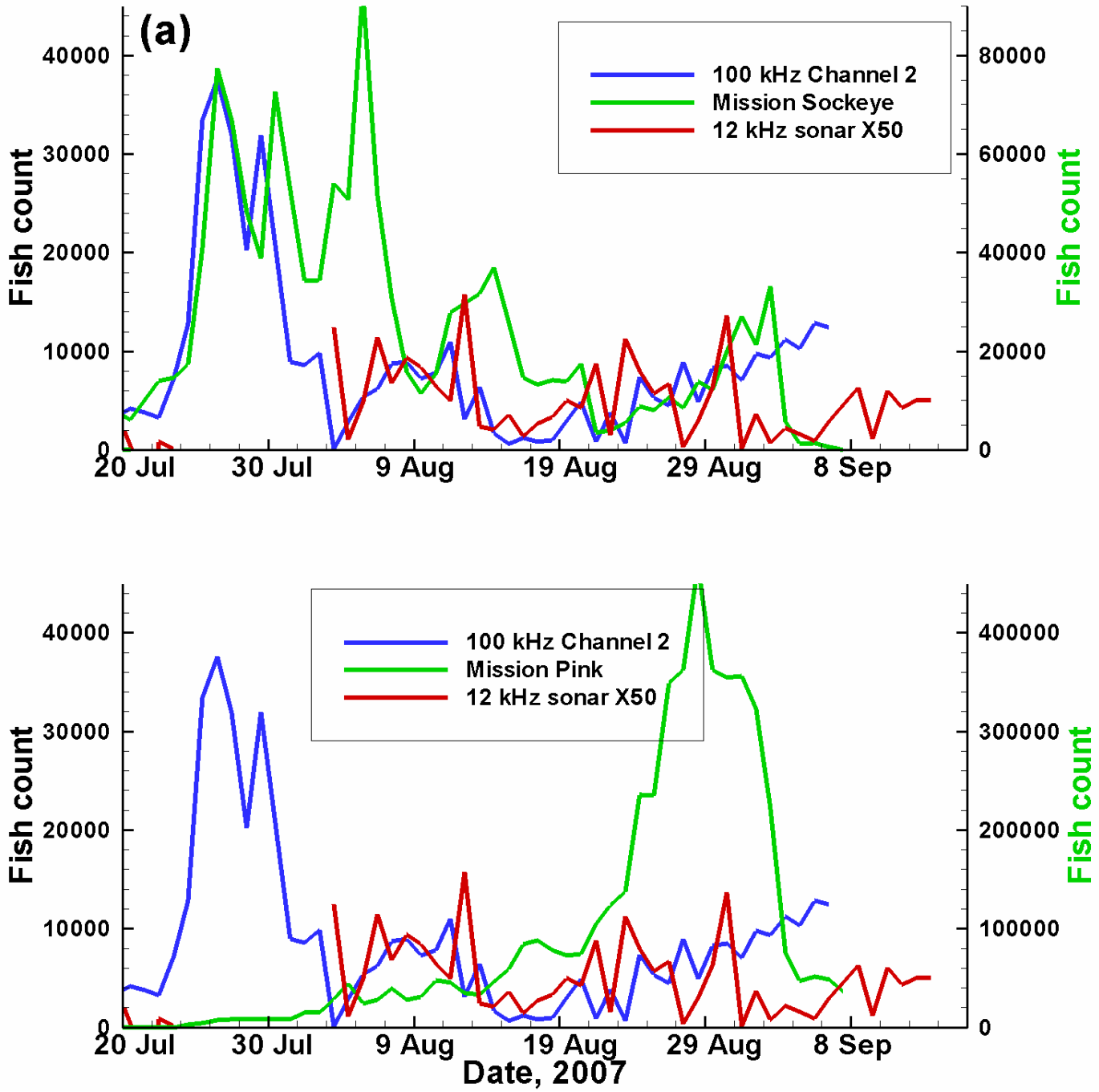

Fig. 24. Same as Fig. 23 except that the Mission fish count estimates have been shifted by 9 days for direct comparisons with the acoustical estimates at Chatham Pt.

Separating sockeye salmon from pink salmon?

Upon comparing typical 12 kHz sonar range profiles from July and August it was discovered that the fish targets in July were typically found in the 300-800 m, whereas they were found in the 50 to 400m range in August (Fig. 25). This correlates to the behaviour differences of sockeye salmon and pink salmon. Pink salmon generally travel close to shore and in large schools.

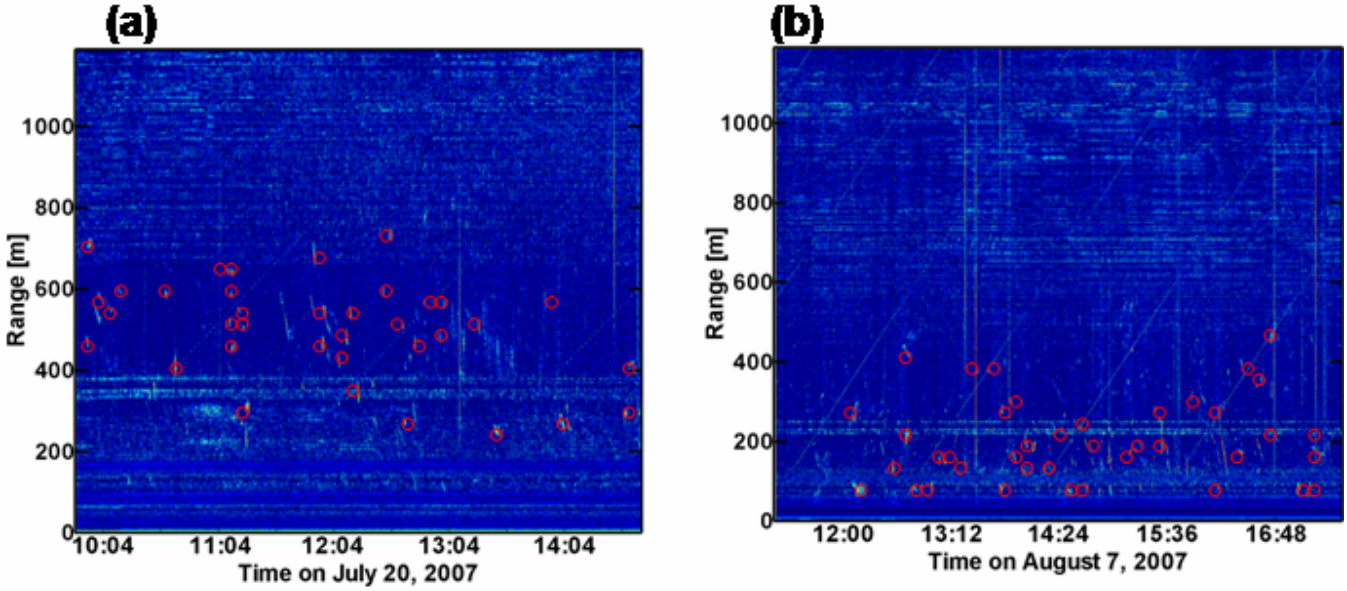

Fig. 25. Fish targets detected by 12 kHz sonar in July (a), and August (b). A majority of the targets have been identified by red circles. There is a clear trend towards finding a majority of the targets closer to shore in August.

This distributional shift between sockeye and pink dominated migrations is consistent with the cross-river distributional shift of fish targets detected at Mission for the two time periods. The two cross-river target distributions in Figure 26 were detected on August 16 (the peak sockeye migration date) and September 9 (the peak pink migration date) at Mission by a mobile sonar system. The sockeye were seen distributed quite evenly across the river with a 50% cross-river quantile interval between 75 and 263 m from the left bank (the south bank). The pink salmon displayed a shore-oriented distribution with a wider 50% quantile interval between 37 and 335 m; the distribution was skewed heavily towards both banks. The true 50% range was likely less than 90 m as the mobile survey system was ineffective in detecting large numbers of pink salmon migrating in nearshore shallow waters.

These significant differences in target range may allow for future species determination without test fishery samples.

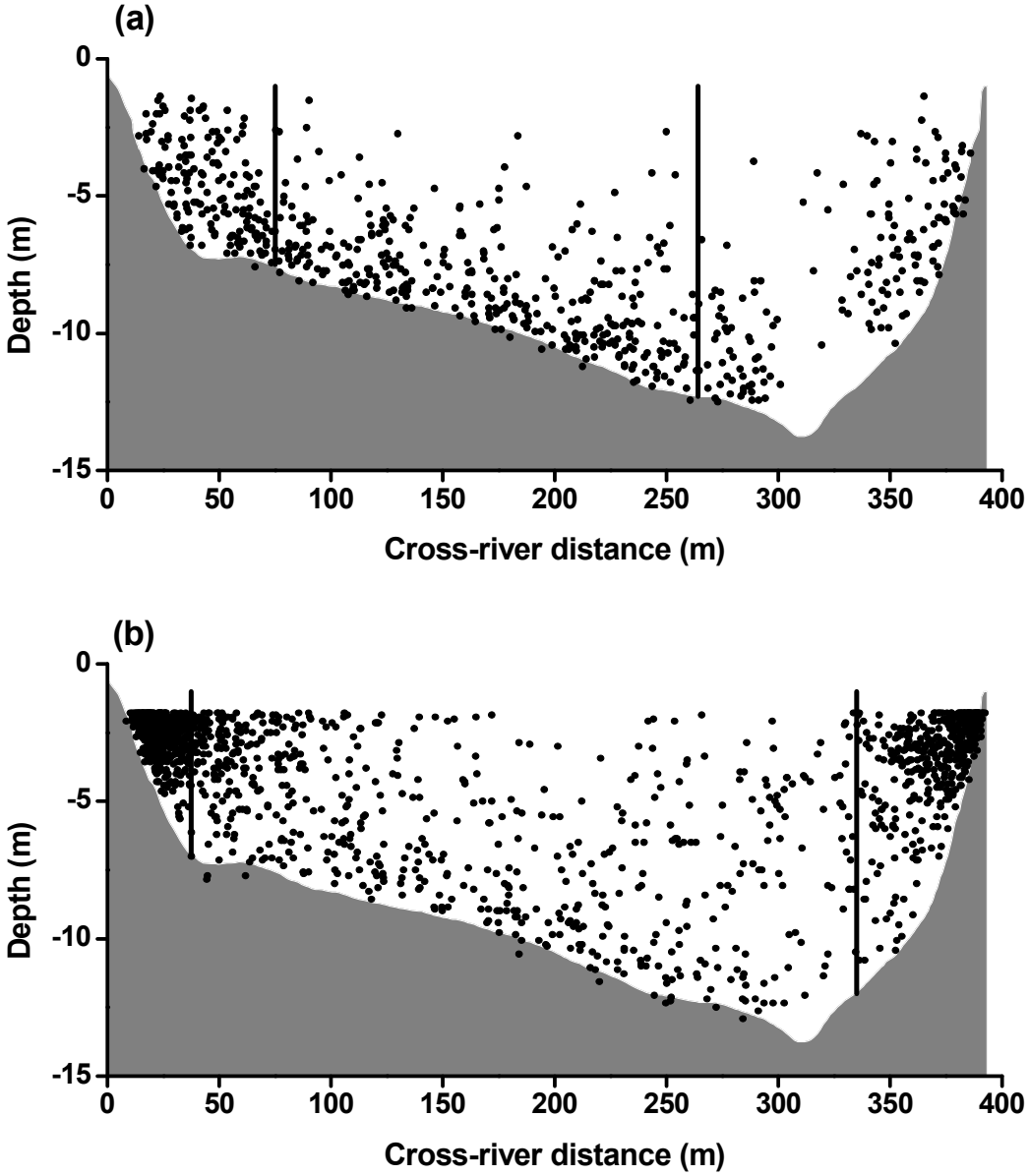

Fig. 26. Cross-river 24-hour cumulative target distributions detected by a 32° single-beam transducer towed by a mobile survey vessel at Mission, B.C. The two vertical lines indicate the 50% quantile range interval of the distribution. The horizontal distance is referenced to a fixed point from the left bank, and the depth is referenced to the daily mean water height. (a) Target distribution on August 16, 2007 (the peak daily sockeye migration in 2007). Total number of detected targets: 668; (b). Target distribution on September 9, 2007 (the peak daily pink migration in 2007). Total number of detected targets: 1600.

DIDSON Results

It was hoped that the DIDSON systems would allow us to verify the targets that were recorded by the stationary acoustic systems. We collected approximately 16 hours of DIDSON data while transecting in the vicinity of Chatham Pt., trying numerous orientations of the DIDSON from looking sideways to looking straight down in the water column. During the early season survey, (sockeye time period) fish targets were only associated with the substrate, and these fish were determined to be rockfish from their body shape and behaviour. We did not detect fish targets in the water column until the later season survey, and then only after all of the DIDSON files were reviewed in the lab. We found only two instances of fish schools in the data recorded during the pink salmon migration period. Still images were made from these data files and are presented in Figures 34 and 35.

We believe that the images in Figs. 27 and 28 are of schools of pink salmon migrating south through Johnstone Straight, as pinks were known to be the predominant species migrating at that time. The images were recorded within 100 m of the shoreline and in an area where sport fisherman were actively fishing. In Figure 27 the small yellow line is drawn to the same length as a typical target in the school. The statistical overview in the bottom left corner of the DIDSON image shows the target to be approximately 55 cm in length, which is within the range we would expect a Fraser River pink salmon to be. This target is approximately 13 m from the transducer and so the DIDSON length measurement is quite accurate at this range (Cronkite et al, 2006). Figure 28 presents another school of fish at approximately 24 m range. It is easier to determine that these targets are fish when the moving images are viewed, as then the undulating swimming motion of the fish is readily observable.

The difficulty in detecting fish targets in the water column was disappointing, but upon further contemplation it is not surprising that the fish were hard to detect. There is an enormous volume of water in Johnstone Straight and the dimensions of the DIDSON beam, along with its shorter-range detection abilities due to its high operating frequency, means that we can cover only a relatively small volume of water. Even if many thousands of fish are present at a point in time, it will still be difficult to detect them unless one chances across a place where they are concentrated. The fish will be easier to detect if they are concentrated for biological reasons, but we were unable to find such places during our surveys. We also believe that the times we surveyed were not at the very peaks of migration and so there were fewer fish present, making detection more difficult. The two fish schools that we did detect provide support for the assumption that the fish are migrating through the 12 kHz and 100 kHz acoustic beams in schools. Very few other targets were detected with the DIDSON system when we were looking at the water column. At various times we detected bubble noise signatures from small vessels, but in general the water column appeared to have very little superfluous noise detectable by the DIDSON system. This provided very clear images of fish targets in the DIDSON beam.

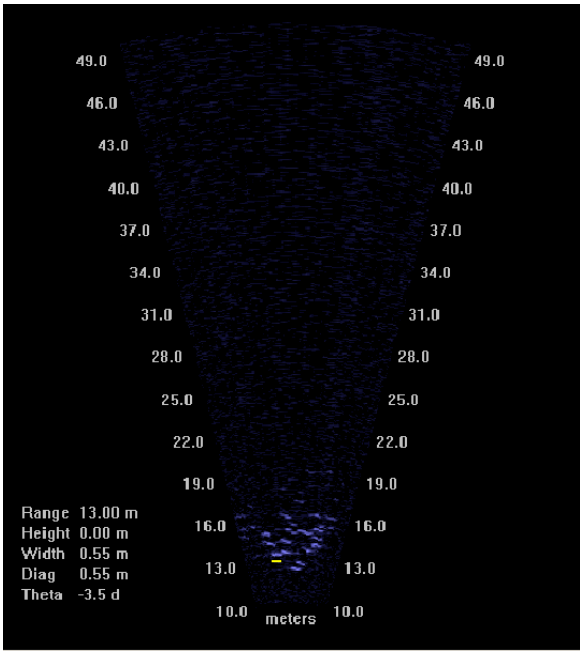

Fig. 27. A Standard DIDSON low frequency still image of a school of fish believed to be pink salmon near Chatham Pt. Low frequency was in use at this point in time to maximise the detection range. The statistics are given in the lower right of the figure for the yellow line drawn on the image. The line shows that the fish images are approximately 55 cm long and at a range of approximately 13 m from the transducer and 3.5º to the left of the axis (Theta). The other listed dimensions are meaningless in this situation as they are for a box outline that would have a height and diagonal measurement, but in this case we have drawn a line to display only the length of the image.

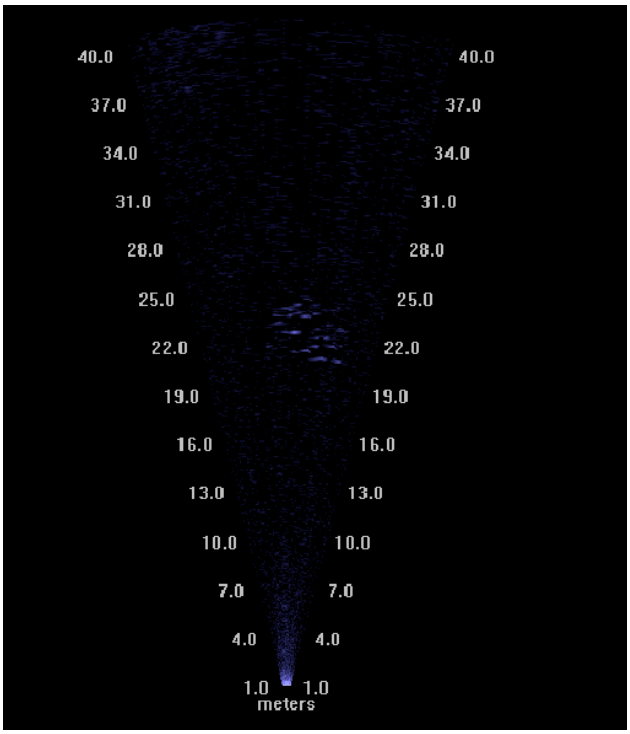

Fig. 28. A Standard DIDSON low frequency still image of a school of fish believed to be pink salmon near Chatham Pt. at approximately 23 m range from the transducer. The fish were similar in size and behaviour to those in Figure 27.

CONCLUSIONS

With a decreasing availability of the important catch per unit effort data from purse seine test fisheries in both Juan de Fuca and Johnstone Straits there is an urgent need to develop alternative information avenues for accurate and timely information on migration abundance and behaviour of salmon returning to the Fraser River from marine waters, which the management of the sockeye salmon fisheries relies on.

The main objective of this project was to determine whether a hydro-acoustic installation in Johnstone Strait can be used to detect and count returning sockeye and pink salmon, headed for the Fraser River system. As a feasibility project, the Johnstone Strait sonar system, deployed at Chatham Pt. lighthouse station was very successful. Though it is not quite ready to be deployed permanently and used as an alternative to test fishing, the project has shown significant potential. Further investigation is required to determine the relationship between the daily fish counts obtained by the sonar system and the true volume of fish travelling through the strait. Also, a method of determining the number of fish in individual schools detected by the mid-range 12 kHz sonar must be developed in order to improve the accuracy of the fish counts. The use of a dual-system, incorporating both a longer range 12 kHz system and a shorter range 100 kHz system is showing promise as a technique to estimate both mid-channel fish and fish travelling close to shore. The possible preference of pink salmon to travel closer to shore than the sockeye salmon may give us a way to separate the abundance estimates of the two species.

The most significant scientific results of the study are that sockeye salmon entering Fraser River were detected approximately 9 days earlier at Chatham Pt., that the fish counts at Chatham Pt. were approximately ½ of the counts at Mission and that the majority of the fish passed Chatham Pt. in a shorter period than at Mission. Another important finding was the possibility that the pink salmon travels closer to shore than the sockeye, something that may make it possible to separate the abundance estimates of these two important species.

As part of this project we also developed an acoustic propagation model for the area. This model is important for proper interpretation of the acoustic data.
A software package to allow for automatic identification of fish targets from both the 12 and 100 kHz sonar data was also developed and tested in this project. The developed processing software also includes a module to use echo-integration to estimate the number of fish in detected schools. However, during this particular study the sonar calibrations were not sufficient to allow for this type of analysis. This would be corrected for in future studies.

With proper system calibrations it will be possible to obtain significantly better estimates of total fish flux by combining both the 100 kHz data (for near range) and 12 kHz data (for longer range). Because of logistical reasons it was not possible to perform a proper calibration of the two systems prior to the deployment at Chatham Pt. this time around.

One of the first attempts at using a DIDSON imaging sonar in the marine environment showed that this type of system can be a useful tool for determining the presence of fish in the Chatham Pt. area but a great deal of time and effort must be spent to detect only a few targets. We feel that the use of the DIDSON for this study did provide some useful information, but that in an ongoing enumeration facility the time required to gain useful data may not be well spent. The DIDSON data cannot be applied in a quantitative manner to the other collected acoustic data, but it may give the researchers a qualitative sense that the acoustics are in fact recording fish traces and not just sources of acoustic noise. The likelihood of detecting salmon with the DIDSON is much higher if the data are collected during the peaks of migration. It may be

most useful to focus on these time periods, and at the ranges where the 12 kHz and 100 kHz systems are most commonly detecting targets. Such systems may also aid in the problem of species identification.

The deployment and recovery of the system went really well. However, corrosion problems resulted in loss of some components after four months in the water. For a more permanent setup these issues will have to be sorted out. However, even a permanent system will have to be recovered occasionally for cleaning and anode replacement. A problem that slipped everybody's mind was the issue of placing high-voltage cables next to sensitive signal cables on dry land. This resulted in the high-voltage signals jumping across and destroying sensitive electronics in other sensors. In any future deployment the solution to this will be to reduce the number of cables crossing land by powering sensitive electronics from an additional pressure housing attached to the tripod itself.

ACKNOWLEDGEMENTS

This project would not have been possible without the great help from a number of people. First of all we want to thank Steve Bergh and Alice Woods, lighthouse keepers at Chatham Pt. lighthouse station, for letting us have access to the buildings and the internet. We also want to thank them for letting us overnight at the station and for some wonderful meals and conversations in their home. This would not have been possible without their support.

We also want to thank Glenna Evans from the Canadian Coast Guard for sorting out the paper work involved in working from the lighthouse station. Ken and Elvis Chickite on the Marinet did a wonderful job in deploying and recovering the tripod at Chatham Pt.
We also want to acknowledge the tremendous effort by Ron Teichrob, Truesolutions Inc., and Scott Rose (DFO/IOS) in putting the system together, getting it deployed, making repairs and finally getting it back at the end of the study.

Grace Kamitakahara, DFO/IOS, helped to process the 12 kHz sonar data and did a great job keeping the link between IOS and our system at Chatham Pt. operational, including downloading of large datasets. We acknowledge the professional help from John Morrison, Vynx Designs Inc., with operating the small boat and collecting data from the waters surrounding the tripod. We want to thank the Canadian Hydrographic Service (CHS) for letting us have access to the multi-beam bathymetric data for the study area, and finally we want to thank Patrick Cummins (DFO/IOS) and the officers and crew on CCGS Vector for getting us the CTD data in March 2007.

REFERENCES

Banneheka, S.G., R.D. Routledge, I.C. Guthrie and J.C. Woodey. 1995. Estimation of in-river fish passage using a combination of transect and stationary hydroacoustic sampling. Can. J. Fish. Aquat. Sci. 52: 335-343.

Blackman, S. S., and R. Popoli, 1999: *Design and Analysis of Modern Tracking Systems*. Artech House Publishers, Dedham, MA.

Bowlin, J., Spiesberger, J., Duda, T., and Freitag, L., 1992: Ocean Acoustical Ray-tracing Software RAY. *Tech. Rep. WHOI-93-10*, Woods Hole Oceanographic Institution, Woods Hole.

Cronkite, G.M.W., Enzenhofer, H.J., Ridley, T., Holmes, J., Lilja, J., and Benner, K. 2006. Use of high-frequency imaging sonar to estimate adult sockeye salmon escapement in the Horsefly River, British Columbia. Can. Tech. Rep. Fish. Aquat. Sci. 2647: vi + 47p.

Ding, L. 1993. Acoustical Studies of Breaking Surface Wave in the Open Ocean. *Ph.D Dissertation*, University of Victoria.

Ding, L. and D. M. Farmer, 1992: A Signal Processing Scheme for Passive Acoustical Mapping of Breaking Surface Waves. *J. Atmos. Oceanic Technol,* **Vol. 9, No. 4**, pp484-494.

Farmer, D. M., M. Trevorrow, and B. Pedersen, 1999: Intermediate Range Fish Detection with a 12-kHz Sidescan Sonar. *J. Acoust. Soc. Am.,* **Vol. 106, No. 5**, pp2481-2490.

A. Ishimaru, Wave Propagation and Scattering in Random Media. Academic Press, New York, 1978, Vols. I and II

Medwin, H. and C. S. Clay, 1998: Fundamentals of Acoustical Oceanography. Academic Press, San Diego.

Simonds, J. and D. Maclennan, 2005: Fisheries Acoustics: Theory and Practice. Blackwell Publishing.

Theodoridis, S. and K. Koutroumbas, 2003: *Pattern Recognition, 2nd edition*, Academic Press.

Xie, Y. 1999: A Range-Dependent Split-Beam Fish Tracking Algorithm and its Application to Tracking Adult Salmon in the Fraser River. *IEEE J. Oceanic Engr***.**

Farmer, D., M. Trevorrow, and B. Pedersen, 1999. Intermediate range fish detection with a 12kHz sidescan sonar, *J. Acoust. Soc. Am.* **106**(5), 2481-2490.

Trevorrow, M., 2001. An evaluation of a steerable sidescan sonar for surveys of near-surface fish, *Fish. Res.* **50**(3), 221-234.

Trevorrow, M., and B. Pedersen, 2000. Detection of migratory herring in a shallow channel using 12- and 100-kHz sidescan sonars, *Aquat. Living Resour.* **13**, 395-401.

Farmer, D., M. Trevorrow, and B. Pedersen, 1999. Intermediate range fish detection with a 12kHz sidescan sonar, *J. Acoust. Soc. Am.* **106**(5), 2481-2490.

Xie, Y. 2000. A range-dependent echo-association algorithm and its application in split-beam sonar tracking of migratory salmon in the Fraser River watershed. IEEE, Journal of Oceanic Engineering, Vol. 25. No. 3, pp. 387-398.

Xie, Y., A. P. Gray, F. J. Martens, J. L. Boffey and J. D. Cave. 2005. Use of Dual-Frequency Identification Sonar to Verify Salmon Flux and to Examine Fish Behaviour in the Fraser River. Pacific Salmon Comm. Tech. Rep.

APPENDIX

Numerical simulation of echo integration

Here we examine the application of echo integration to the estimation of fish passage associated with individual echo traces, which may contain multiple fish. Echo integration relies on the assumption that the integrated intensity backscattered from an assemblage of targets can be considered equal the sum of the echo intensity from each individual target that would have been received in the absence of the other targets. If this assumption holds, the total intensity is proportional to the amount of the targets. Multiple scattering, shadowing, and coherent interference have been identified as factors that may invalidate the underlying linearity assumption. The first two may be negligible at low target densities, but whether coherent interference can be ignored remains an open question. For coherent interference to disappear, it is required that targets be randomly distributed in an observation area such that over each signal transmission, there is no constant phase relation among the echoes. If the requirement is satisfied, the coherent interference can be smoothed out by averaging the total received signal over transmissions.

Figure 13 indicates that fish pass through the observation view in groups. At ranges 400-600m the fish groups may stay in the beam for 1-2 min. The duration of stable backscattered signals may be less than 1 min. At a ping rate of 2 pings per second, whether there are sufficient pings for averaging to remove coherent interference becomes a question. If the answer to the first question is positive, then a second question is how to estimate the fish passage for echo traces such as those in Fig. 13, given all possible information we may extract from the data.

Model formulation

Consider a group of N individual targets, ensonified by an acoustic pulse of duration t_d. To the first order, the backscattered pressure can be expressed as

$$p_s(t) = \sum_{n=1}^{N} p_s(t,n) = \sum_{n=1}^{N} D_t(\mathbf{r}_n) D_r(\mathbf{r}_n) \frac{e(t-\tau_n) S(\mathbf{r}_n)}{r_n^2} \exp\{-2[\alpha r_n]\}, \qquad \text{(A1)}$$

where D_t and D_r are the beam response of the transmitting and receiving transducer respectively. The factor

$$[\alpha r_n] = \int_0^{r_n} \alpha(x)dx \qquad \text{(A2)}$$

represents accumulated attenuation up to range r_n, with $\alpha(x)$ being the range-dependent attenuation factor. $e(t)=exp(i\omega t)w(t)$ is the transmitted waveform, and $\tau_n = 2r_n/c$ is the delay of echo from the nth target, where $S(\mathbf{r}_n)$ is the scattering function of the nth target, which depends on the location and orientation of the target. Note also that in Eq. (A1), we set the source level to unity. The echo-squared integration is defined as

$$I = \int_{t_1}^{t_2} |p_s(t)|^2 dt = \sum_{n=1}^{N} \int_{t_1}^{t_2} |p_s(t,n)|^2 dt + \sum_{m=1}^{N} \sum_{m=n+1}^{N} \int_{t_1}^{t_2} \left[p_s(t,m) p_s^*(t,n) + p_s^*(t,m) p_s(t,n) \right] dt \,, \qquad \text{(A3)}$$

where the integration is performed over a time interval between t_1 and t_2 which corresponds to a range gate between $R_1(= ct_1 /2)$ and $R_2(= ct_2 /2)$. In Equation (A3), the first term on the right-handed side is the incoherent component, expressed as

$$I_d = \sum_{n=1}^{N} \frac{b^2(\mathbf{r}_n)\left|S(\mathbf{r}_n)\right|^2}{r_n^4} \exp\{-4[\alpha r_n]\} \int_{t_1}^{t_2} \left|w(t-\tau_n)\right|^2 dt \,. \tag{A4}$$

where $b(\mathbf{r}_n) = D_t(\mathbf{r}_n) \times D_r(\mathbf{r}_n)$, and the second term is the coherent component, expressed as

$$I_c = 2\sum_{m=1}^{N}\sum_{n=m+1}^{N} \frac{b(\mathbf{r}_m)b(\mathbf{r}_n)}{r_m^2 r_n^2} \mathrm{Re}\left[S(\mathbf{r}_m)S^*(\mathbf{r}_n)\exp\{i2k(r_m - r_n)\}\right] \exp\{-2[\alpha r_m] - 2[\alpha r_n]\} \int_{t_1}^{t_2} w(t-\tau_m)w^*(t-\tau_n)dt \tag{A5}$$

If the pulse width t_d is much smaller than the interval t_2 - t_1, then almost all the targets contributing to the integral will be bounded by ranges $ct_1 /2$ and $ct_2 /2$. In this case, it can be shown

$$GT(\tau_n) = \int_{t_1}^{t_2} \left|w(t-\tau_n)\right|^2 dt \approx t_d \,, \tag{A6}$$

and

$$GT(\tau_m, \tau_n) = \int_{t_1}^{t_2} w(t-\tau_m)w^*(t-\tau_n)dt \approx \begin{cases} t_d - \left|\tau_m - \tau_n\right| & \left|\tau_m - \tau_n\right| \le t_d \\ 0 & otherwise \end{cases} . \tag{A7}$$

The incoherent and coherent components, I_d and I_c, depend on the target positions which may be considered randomly distributed. Monte Carlo simulation can be performed to calculate the components separately under various conditions.

Estimation of the number of targets

We now investigate the problem of estimating the total number of targets based on the ensemble average of the incoherent component. For a group of N targets, it can be shown (see Ishimau (1978) for details) that

$$\left\langle I_d \right\rangle = \int \left[I_d\right]_\xi \frac{\rho(\mathbf{r}_1)...\rho(\mathbf{r}_N)}{N^N} d\mathbf{r}_1 ... d\mathbf{r}_N \,, \tag{A8}$$

where $\rho(\mathbf{r}_1)$,.., $\rho(\mathbf{r}_N)$ are the target density at locations $\mathbf{r}_1$ ... $\mathbf{r}_N$. $[I_d]_\xi$ is the average of I_d over all other characteristics except for positions of the targets. In this application, these characteristics include orientation and size, and only the scattering function needs to be averaged with respect to size and orientation. Applying this general approach to our problem, we obtain

$$\langle I_d \rangle = \sum_{n=1}^{N} GT(\tau_n) \int \frac{b^2(\mathbf{r}_n)[\sigma(\mathbf{r}_n)]_\xi}{r_n^4} \exp\{-4[\alpha r_n]\} \frac{\rho(\mathbf{r}_n)}{N} d\mathbf{r}_n$$
$$= t_d \int \frac{b^2(\mathbf{r})[\sigma(\mathbf{r})]_\xi}{r^4} \exp\{-4[\alpha r]\} \rho(\mathbf{r}) d\mathbf{r} \quad , \tag{A9}$$

where we have used $\int \rho(\mathbf{r}_n) d\mathbf{r}_n = N$, and $\sigma(\mathbf{r})=|S(\mathbf{r})|^2$ (cross section).

If we assume the targets are uniformly distributed within the space they occupy, then we have

$$\langle I_d \rangle = \rho t_d \int_{Vo} \frac{b^2(\mathbf{r})[\sigma(\mathbf{r})]_\xi}{r^4} \exp\{-4[\alpha r]\} d\mathbf{r} \,, \tag{A10}$$

where the integration is performed over the occupied volume *Vo*. If we further assume that targets are concentrated within a compact region bounded by a range gate, then we can approximate the calculation of the number of targets as

$$N = \rho \int_{Vo} r^2 dr d\Omega = \frac{1}{3} \rho (R_2^3 - R_1^3) \Delta\Omega \approx \rho R^2 \Delta R \Delta\Omega \,, \tag{A11}$$

where $\Delta\Omega$ is the solid angle covering the cluster of targets and ΔR is the thickness of the region. Similarly,

$$\langle I_d \rangle \approx \rho t_d \frac{\Delta R}{R^2} \exp\{-4[\alpha R]\} \int_{\Delta\Omega} [\sigma(\mathbf{r})]_\xi b^2(\Omega) d\Omega \,. \tag{A12}$$

The scattering function depends on incident angle, which is a function of the orientation of a target and the position of the target with respect to the transducer center. In order to estimate the density from the incoherent intensity, we have to do one more approximation here. We replace the cross section (square of scattering function) with its average over a range of incident angle. This range of incident angle can be determined by the ranges of the target position and orientation. Then we can estimate the number of targets in the sampling volume using

$$N \approx \frac{\langle I_d \rangle R^4}{t_d \overline{\sigma}} \frac{\Delta\Omega}{\int_{\Delta\Omega} b^2(\Omega) d\Omega} \exp\{4[\alpha R]\} . \tag{A13}$$

Numerical simulation procedure

The Monte Carlo simulation procedure for this model consists of the following four steps:

1. Randomly generate N targets within a sampling volume. Each target has an initial velocity (3D), with its initial orientation aligned with the velocity; (The initial positions of the targets may be completely uniform distributed in the sampling volume, or may form more or less parallel structures with small perturbations.)

2. After each acoustic transmission, move each target to a new position determined by its velocity and the transmission, or ping, rate, and obtain another velocity; (If a target moves out of the sampling volume, allow another one to move in from the opposite side of the exit location. In this way, N is kept constant.)
3. For each ping calculate the backscatter from an individual target based on its position relative to the source and its orientation, which is the same as the direction of the velocity; (A prolate spheroid model can be used. For simplicity, assume a single length for all targets. This assumption allows rapid computation of the scattering function of each target by creating a look-up table of the scattering function versus incident angle.)
4. Finally, the calculation of the backscatter is repeated for several realizations of N random scatterers, or targets (e.g. salmon).

Results of ping averaging

In the simulation we calculate the echo intensity for each ping, yielding a sequence of values $\mathbf{I} = [I_1, I_2, \ldots, I_K]$. Then the same simulation is run for a number of realizations, leading to a sequence of vectors $\mathbf{X} = [\mathbf{I}_1, \mathbf{I}_2, \ldots \mathbf{I}_M]'$. Then we create a sequence of ping-averaged echo intensity:

$$\bar{I}(l,k) = \frac{1}{k}\sum_{j=1}^{k} I(l,j) \quad k = 1,2,\ldots N \ , \tag{A14}$$

where l=[1, 2, …, M] is the index of realizations. We apply this operation to both total intensity and incoherent intensity, and then normalize the total intensity by the incoherent intensity:

$$r(l,k) = \frac{\bar{I}_{tot}(l,k)}{\bar{I}_d(l,k)} \quad k = 1,2,\ldots K; \quad l = 1,2,\ldots, M \ . \tag{A15}$$

Now with this data matrix, we can analyze statistics of simulation runs.

Figures A1 and A2 show the mean and standard deviation (with respect to realizations) of the ratio for varying ping averaging and for different target densities. Using 20 ping averaging, the mean converges to around 0 dB (one). For one particular realization, the ratio will not be zero dB, as shown in Fig. A2, which indicates the standard deviation is still 0.6dB. However, as it can be seen from Fig. A2, the standard deviation drops sharply as the number of pings increases from 1 to 5, and then gradually decreases as the number of pings continues to increase. Figure A1 also indicates that the convergence starts at 5 pings.

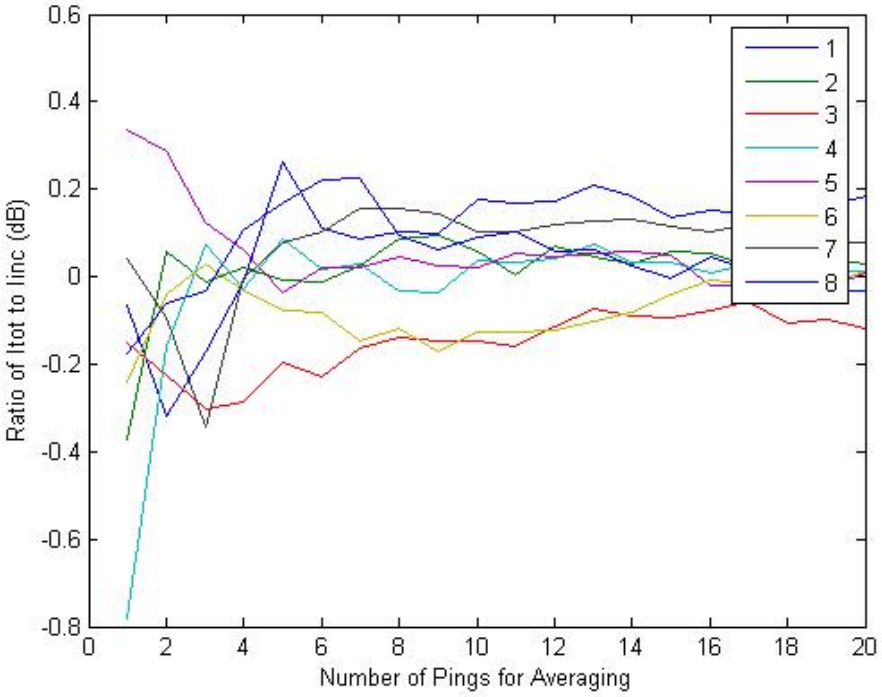

Fig. A1. Mean of the ratio of total intensity to incoherent intensity versus the number of pings used for ping to ping averaging. Different curves represent the results for different numbers of targets (legends 1 to 8 represent the smallest to largest number of targets).

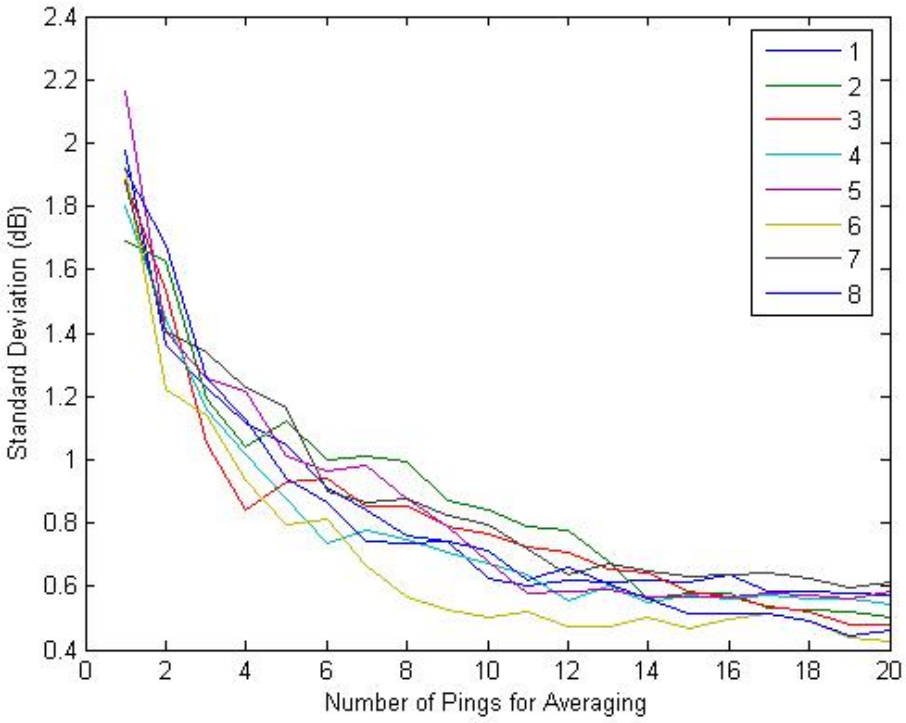

Fig. A2. Standard deviation of the ratio of total intensity to incoherent intensity versus the number of pings used for ping to ping averaging. Different curves represent the results for different numbers of targets (legends 1 to 8 represent the smallest to largest number of targets)..

Results of target number estimation

We now consider the situation where a school of fish move across the beam. If the fish are assumed to move nearly straight across the beam, then we can expect that the total intensity will rise and fall. Of course, due to coherent interference, the rise and fall trend will not be smooth; there will be interference patterns embedded in the general trend. Such a pattern is evidenced in data as shown in Fig. A3 which shows a plot of echo intensity versus time for the data within the red box in Fig. 13. The echo intensity is integrated over the ranges bounded by the box. The red line is the result of a running average filter with order of 5. The choice of the filter order is based on our simulation result.

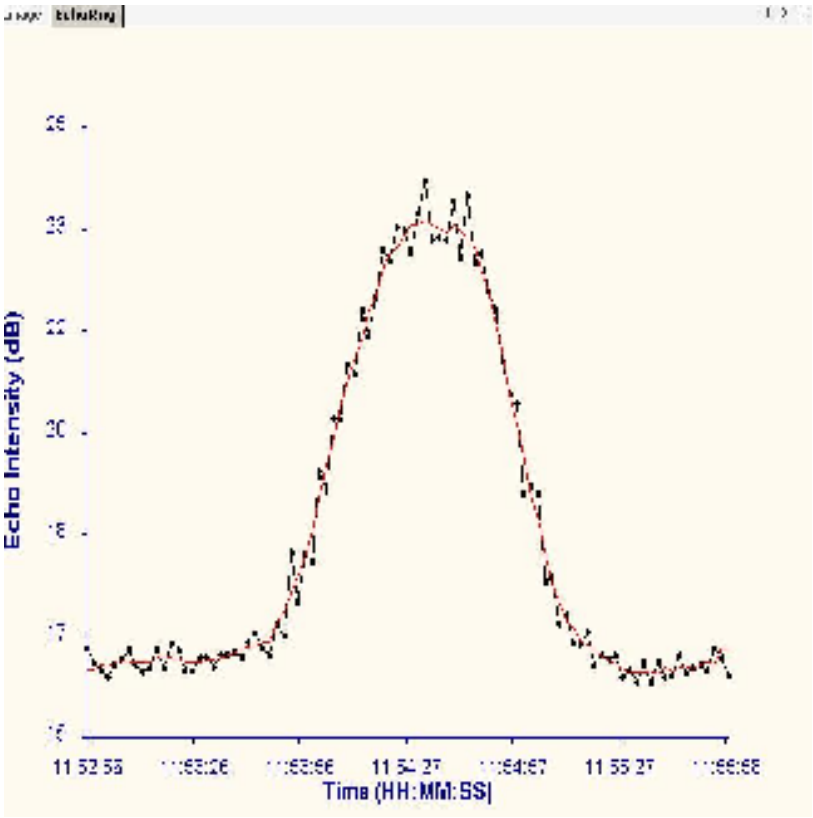

Fig. A3. Integrated echo intensity versus time for the data within the red box in Fig. 13. The echo intensity is integrated over the ranges bounded by the box. A moving smoothing filter of order 5 was applied to the data as shown by the red line.

The pattern can also be simulated, by allowing a group of targets to move from one side of the beam to the other (in this case, we do not add targets to maintain a constant number of targets in the beam). We then calculate the total intensity as a function of time. Figure 18 shows an example of such simulation, where a group of 1281 targets move straight across the beam at a speed of 0.5m/s. The simulation was repeated for

30 realizations. The green lines are the results of a running average filter of order 5.

In order to estimate the number of targets using Eq. (A13), we consider the configuration of the 12kHz sonar, which is a line array of 40 elements, with a horizontal beamwidth of 2.6^0, and an almost uniform vertical beam. This forms a separable two dimensional beam. We need to integrate the beam pattern over the solid angle covering the area occupied by targets. We further assume that targets are in a compact group concentrated around the center of the horizontal beam. In this case, we expect that the received intensity reaches its maximum as the targets move across the beam, as indicated by the peak of the smooth curves in Fig. A4. The vertical beam is very wide so it should cover fish groups in most cases.

As a simplest approximation, Eq. (A13) can be simplified to

$$N \approx \frac{\langle I_d \rangle R^4}{t_d \overline{\sigma}} \frac{\Delta\theta}{\int_{\Delta\theta} b_H{}^2(\theta) d\theta} \exp\{4[\alpha R]\}, \qquad \text{(A16)}$$

where $\Delta\theta$ is the beam angle covering the target area, and $b_H(\theta)$ is the horizontal beam pattern. Here we assume that the vertical beam is uniform with our integration space. More elaborate methods can be applied to the integration over the solid angle, but the largest uncertainty in this model is the mean cross section, which can have large variability and is data dependent. So we feel this simple approach is sufficient for our preliminary analysis.

In the simulation results of Fig. A4 and Fig. A5, we assume that the target region is covered by the 3dB horizontal beamwidth. Using the peak value of the smooth curves in Fig. A4, we can estimate the number of targets. For the 30 realizations, the maximum, minimum, and mean of the estimates are 1795, 868, and 1237, compared with the true value of 1281. Figure A5 shows the histogram of the estimates.

Figure A6 shows another example of the simulation, which has a population of 180. The maximum, minimum, and mean of the resulting estimates are 213, 110, and 167. Figure A7 shows the histogram of the estimates.

In real application, one uncertainty is the region covered by a fish school. If the fish school moves across the horizontal beam nearly perpendicularly, then it is possible to estimate the length of the school based on such time series as in Fig. A3 and swim speed (if it can be obtained from other sources). We further investigate this issue in the future.

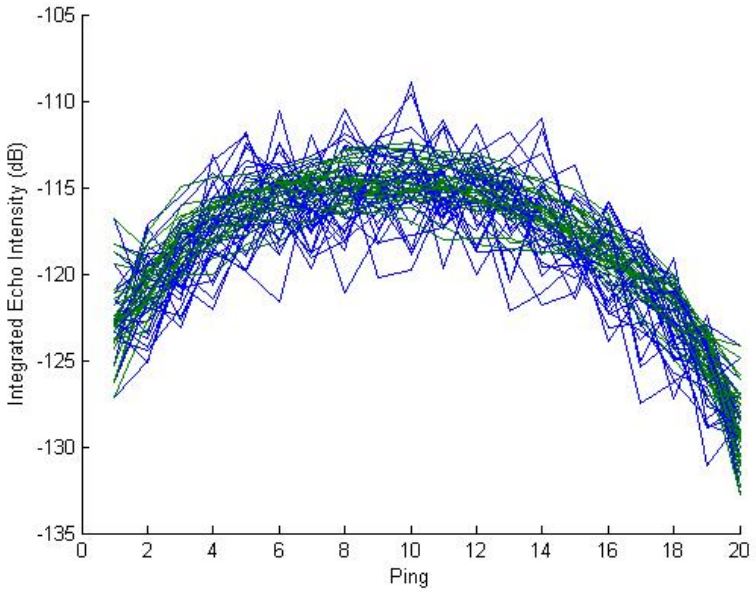

Fig. A4. Integrated echo intensity versus ping number for simulated data of 1281. A moving smoothing filter of order 5 was applied to the data as shown by the green lines. The simulation was repeated 30 times.

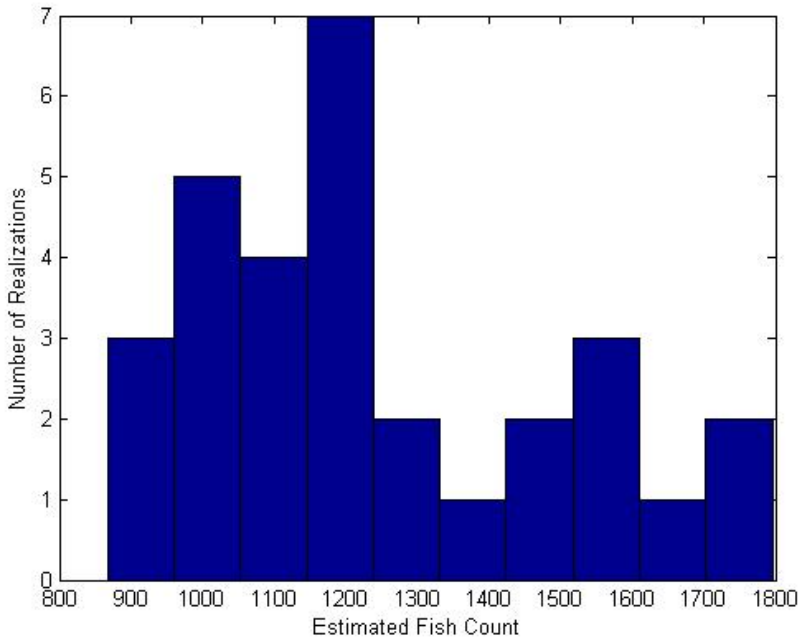

Fig. A5. Histogram of 30 estimates of the number of targets based on the peak value of the smoothed integrated echo intensity in Fig. A4. The true number is 1281.

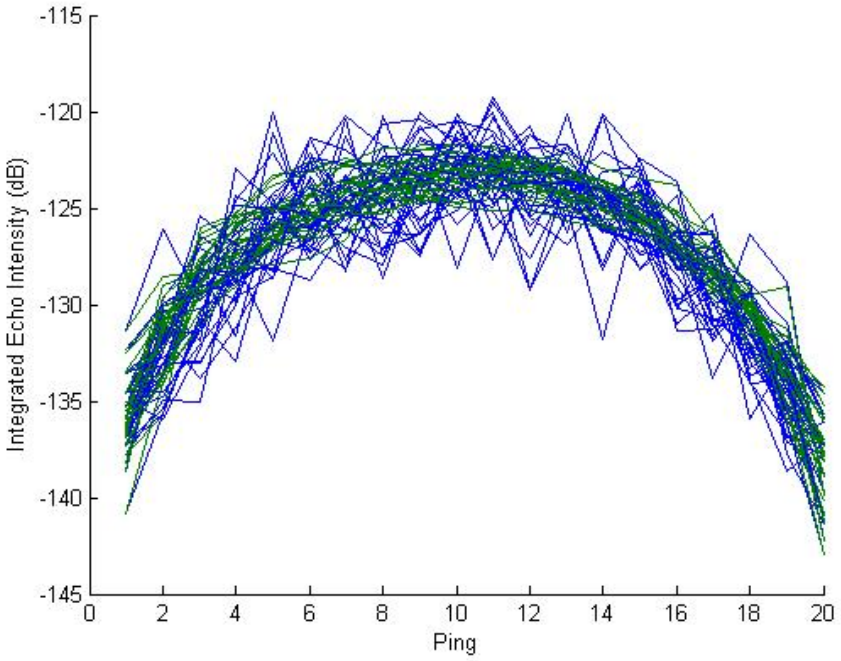

Fig. A6. Integrated echo intensity versus ping number for simulated data of 180. A moving smoothing filter of order 5 was applied to the data as shown by the green lines. The simulation was repeated 30 times.

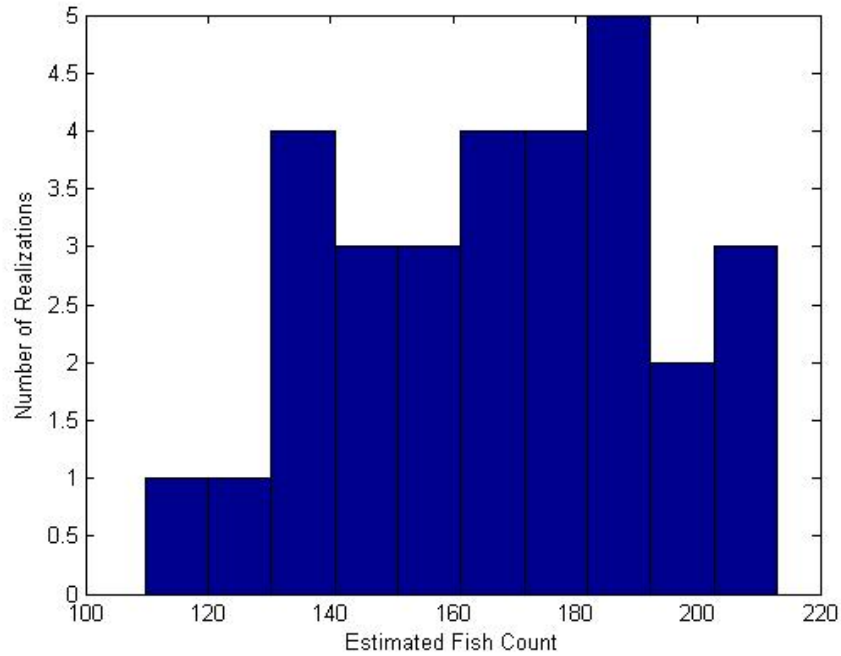

Fig. A7. Histogram of 30 estimates of the number of targets based on the peak value of the smoothed integrated echo intensity in Fig. A6. The true number is 180.